Determination of causal relationships between time series and applications to neural data

Zoltán Somogyvári

Research Centre for Physics of the Hungarian Academy of Sciences
Department of Theory

Determination of causal effects in time series

Is there any possibility to identify directed causal relationships from two data series, with unknown origin, without further experimentation?

We surely can measure correlation, but correlation and causality
are different things. Moreover correlation is a symmetrical relation
while causality can be unidirectional.

Is there a way to infer the directional causality,
to distinguish the bidirectional (circular) causality or to reveal hidden common cause?

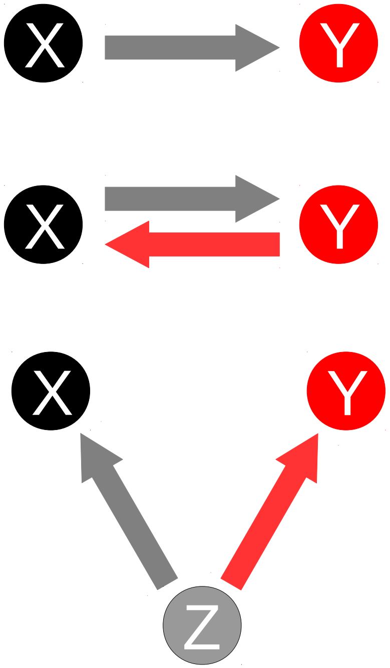

Granger-causality

The original idea of predictive causality came from Norbert Wiener

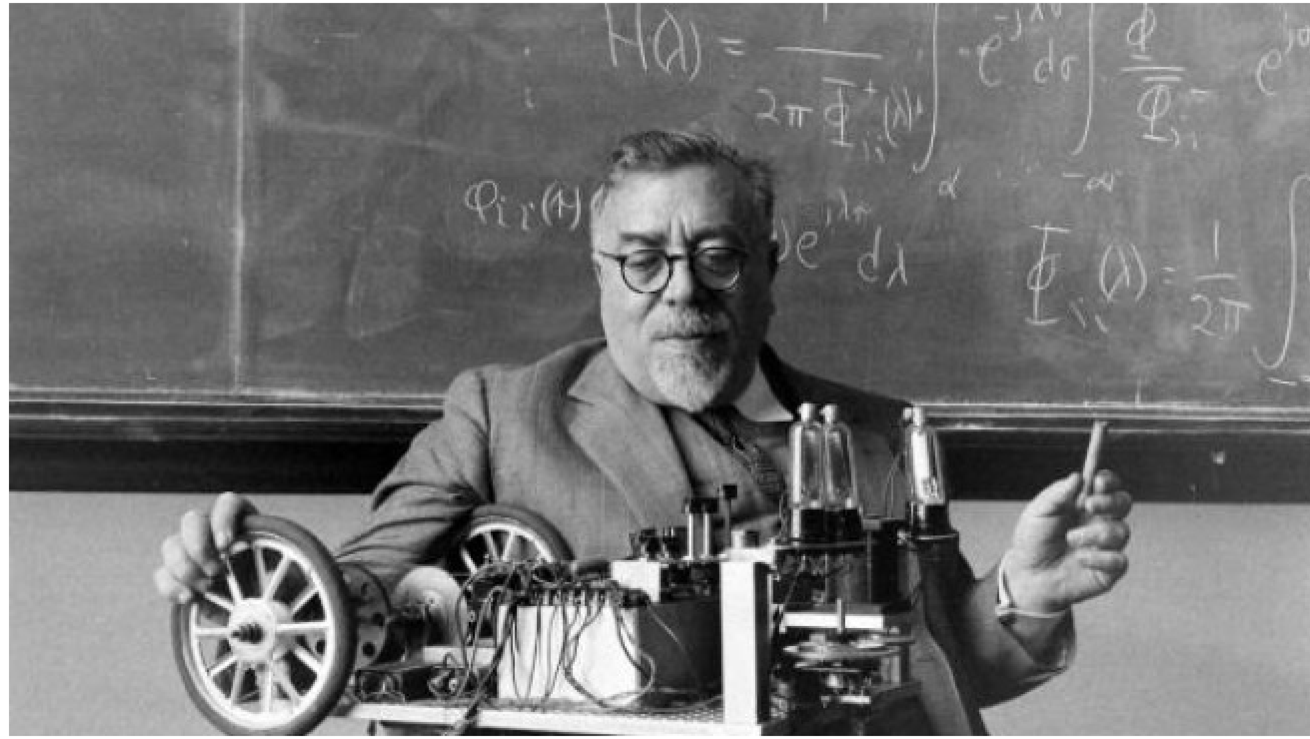

x → ***y***, if the inclusion of past ***x*** values improves the prediction quality on ***y***

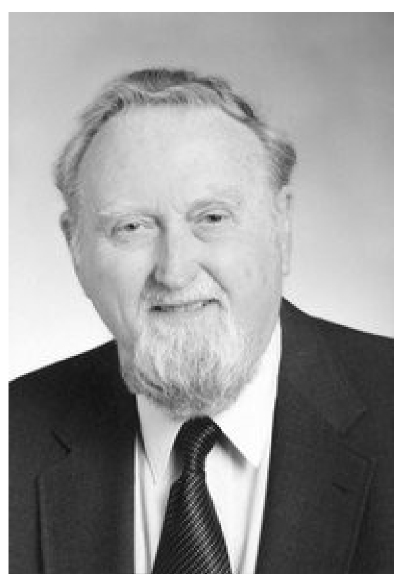

Clive Granger implemented it via autoregressive linear models in 1969

Nobel price in Economic Sciences 2003

Problems with the Granger-causality

It is sensitive to the model used for the prediction. The limitations of linear autoregressive models can be ameliorated by using nonlinear extensions, kernel solutions or model free transfer entropy method.

But, the predictive causality principle can not reveal circular causal relationships!

The predictive causality measures the information added by the second time series, but in case of circular coupling, the information contained by the second data series is already available in the system's own past.

Cross Convergence Map:
A new framework for causality analysis

A new model-free approach, promising:

- Detection of circular causality
- Detection of nonlinear coupling

Detecting Causality in Complex Ecosystems

George Sugihara,[1*] Robert May,[2] Hao Ye,[1] Chih-hao Hsieh,[3*] Ethan Deyle,[1] Michael Fogarty,[4] Stephan Munch[5]

Science **338**, 496 (2012)

It utilizes the Taken's time delay embedding theorem:

The trajectory reconstructed in the state space is topologically equivalent With the trajectory of the system's original trajectory in its real space.

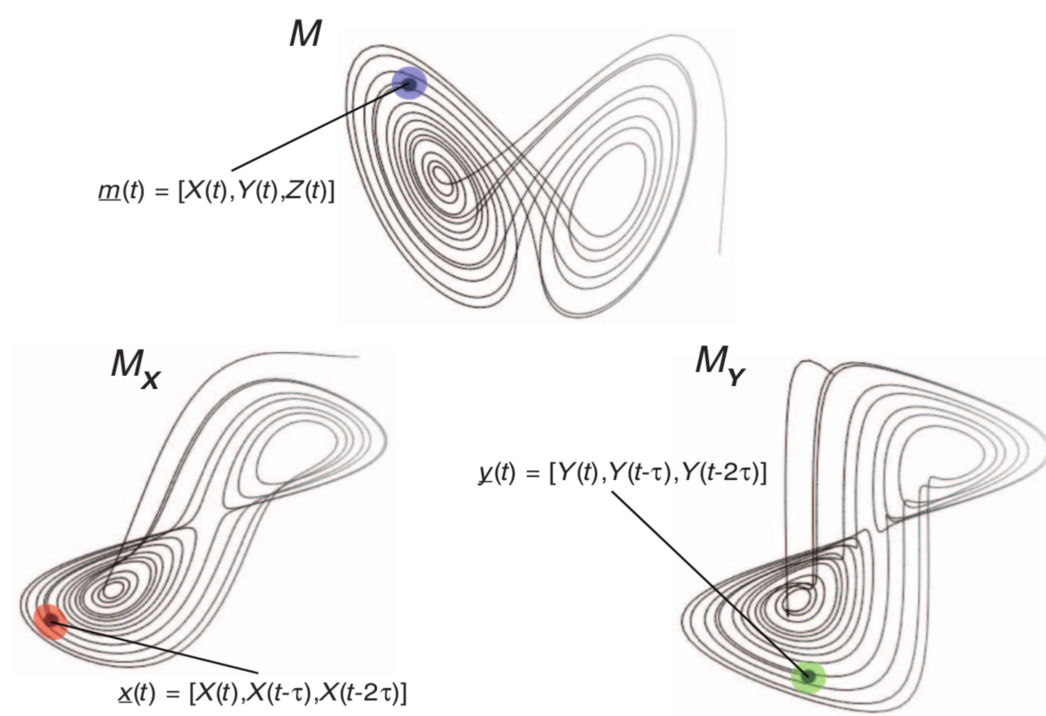

Cross Convergence Map:
A new framework for causality analysis

- Sugihara’s method is based on that the consequence is an observation of the cause, thus the cause can be reconstructed from the consequence.
- Points that are neighbors in the state-space of the consequence should be neighbors in the state space of the cause as well.
- This topology preserving property can be tested by the cross mapping method.

Detecting Causality in Complex Ecosystems

George Sugihara,[1]* Robert May,[2] Hao Ye,[1] Chih-hao Hsieh,[3]* Ethan Deyle,[1] Michael Fogarty,[4] Stephan Munch[5]

Science **338**, 496 (2012)

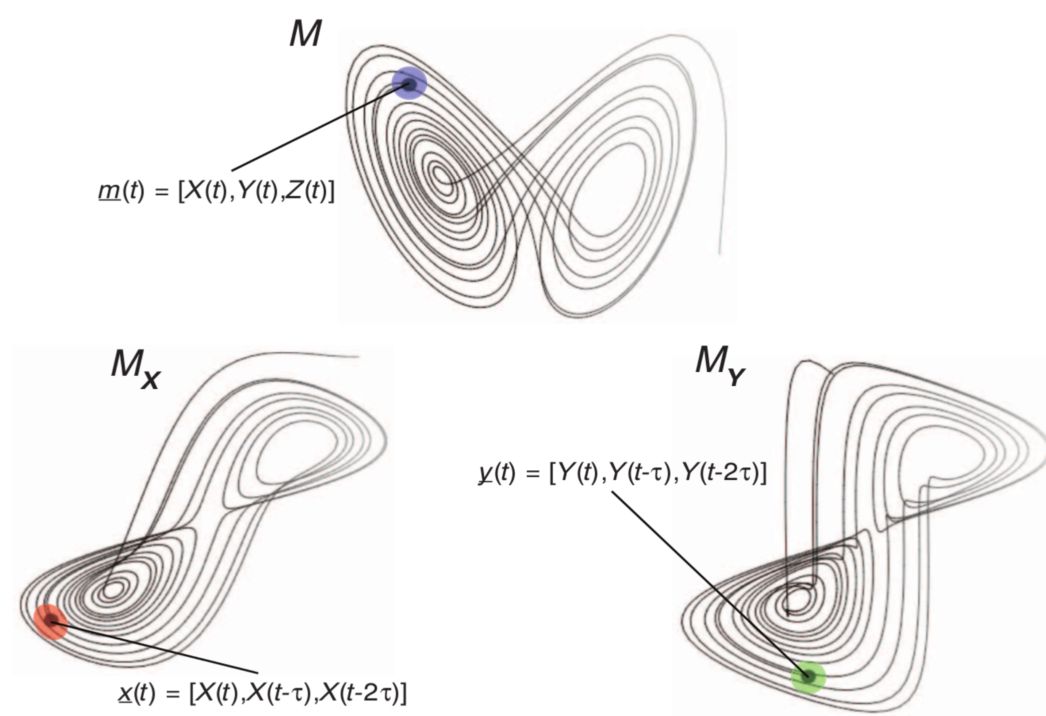

Our first model system: The logistic map

$x_{t+1} = r\, x_t(1-x_t)$

A one dimensional, discreet-time dynamical system implementing stretching an folding transformations.

It can exhibit different dynamical behavior, from stable fixpoint, through periodic oscillations to chaos, depending on the parameter r.

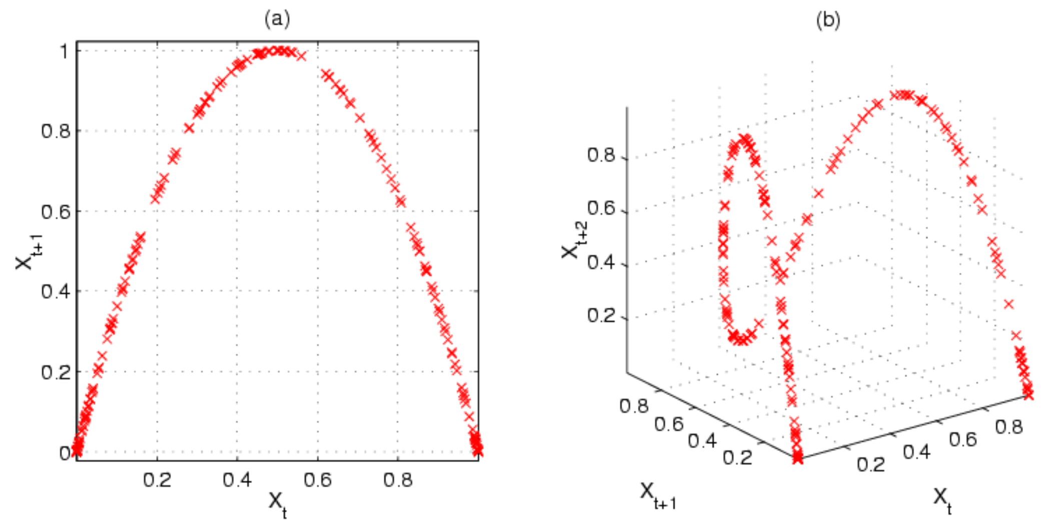

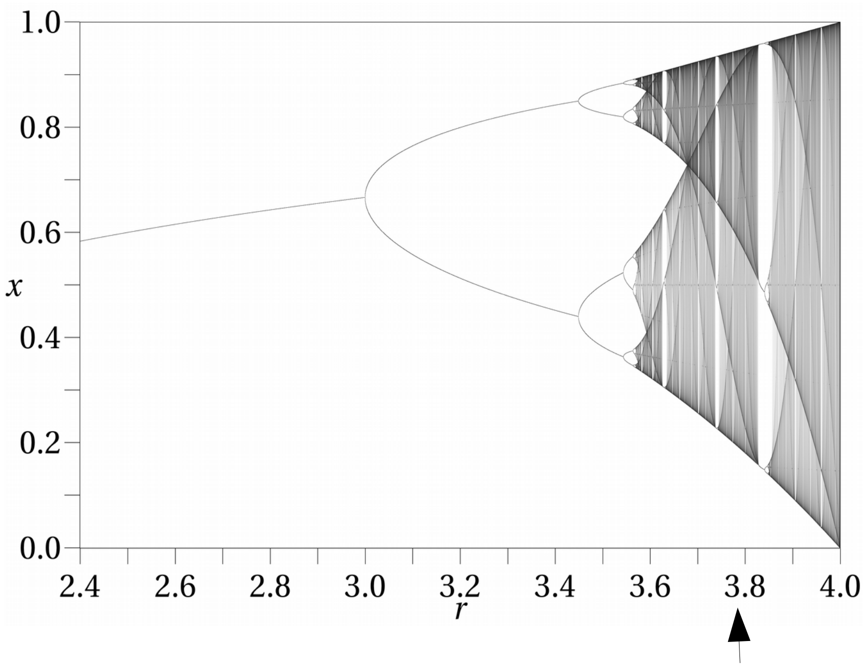

We choose r = 3.8 which ensures chaotic behavior.

Two coupled logistic maps

Case I.: Circular, nonlinear coupling

$x_{n+1}=r_x x_n((1-x_n)+b_{yx}y_n)$

$y_{n+1}=r_y y_n((1-y_n)+b_{xy}x_n)$

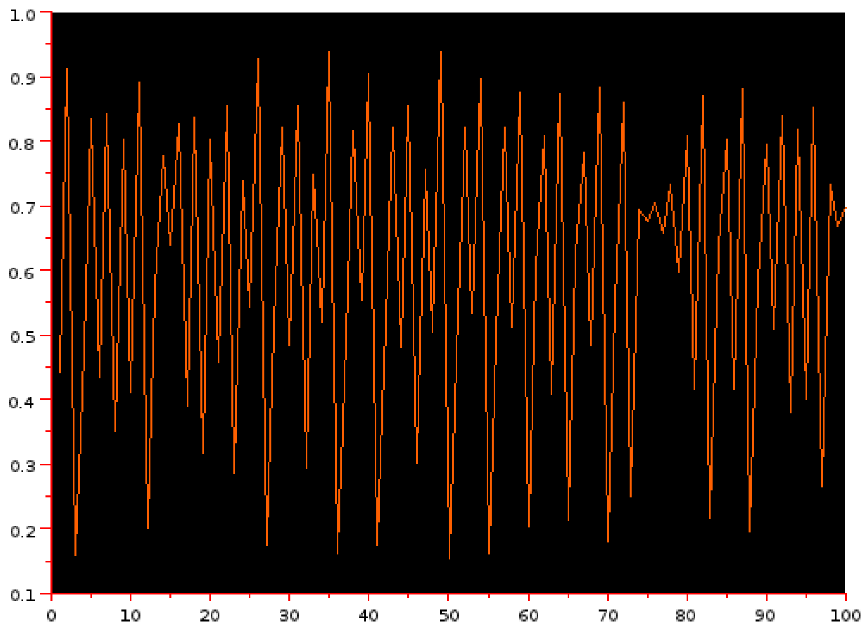

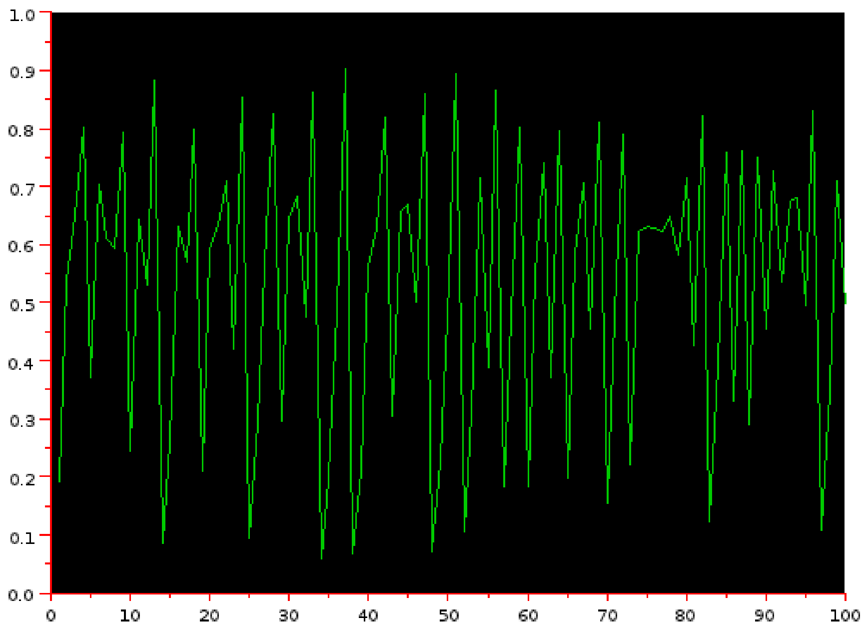

$r_x=r_y=\mathbf{3.8}$ so both maps are in the chaotic regime

Phase-space reconstruction based on delayed maps

$x_{n+1}=r_x x_n((1-x_n)+b_{yx}y_n)$

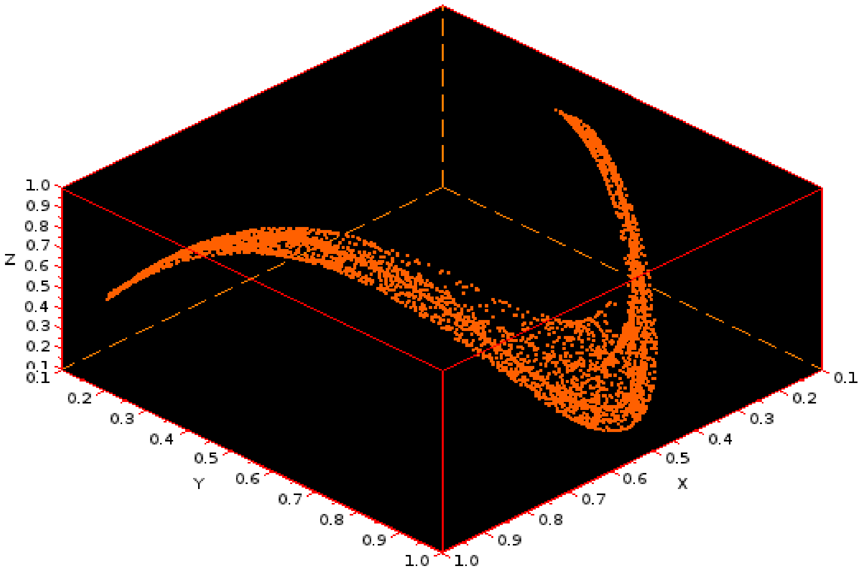

Reconstructed state-space from the first data series in 3 embedding dimension

$y_{n+1}=r_y y_n((1-y_n)+b_{xy}x_n)$

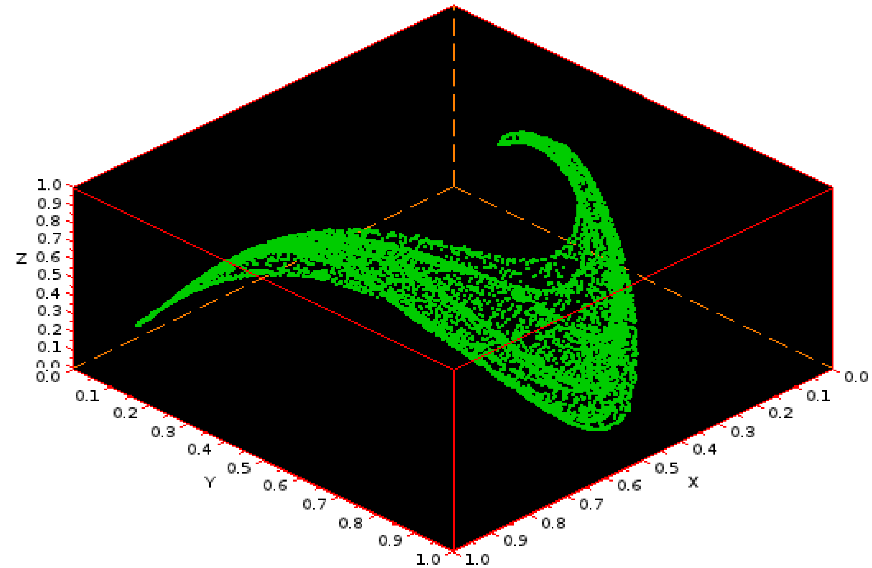

Reconstructed state-space from the second data series in 3 embedding dimension

Both dataset formed a 2D manifold in the 3D embedding space.

Existence of a diffeomorphism

In case of causal connections, the reconstructed manifold sholud be topologically equivalent according to the Takens' theorem. But, how to test it?

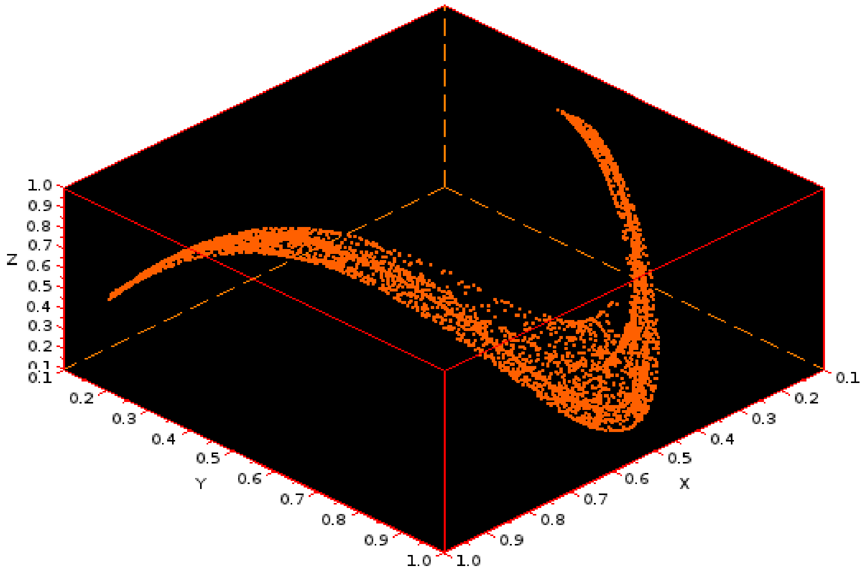

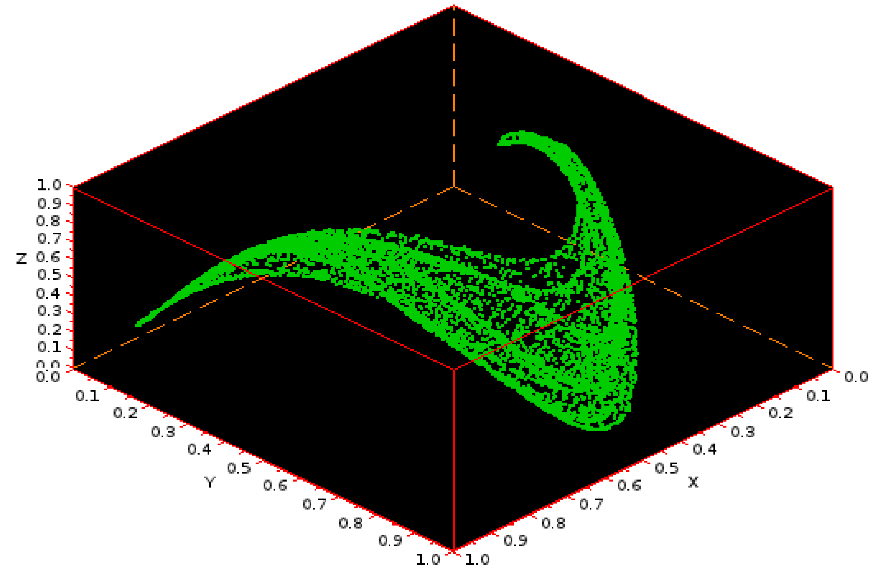

Reconstructed state-space from the first data series in 3 embedding dimension

Reconstructed state-space from the second data series in 3 embedding dimension

Both dataset formed a 2D manifold in the 3D embedding space.

Sugihara's method: Convergent Cross mapping

Choose a point!

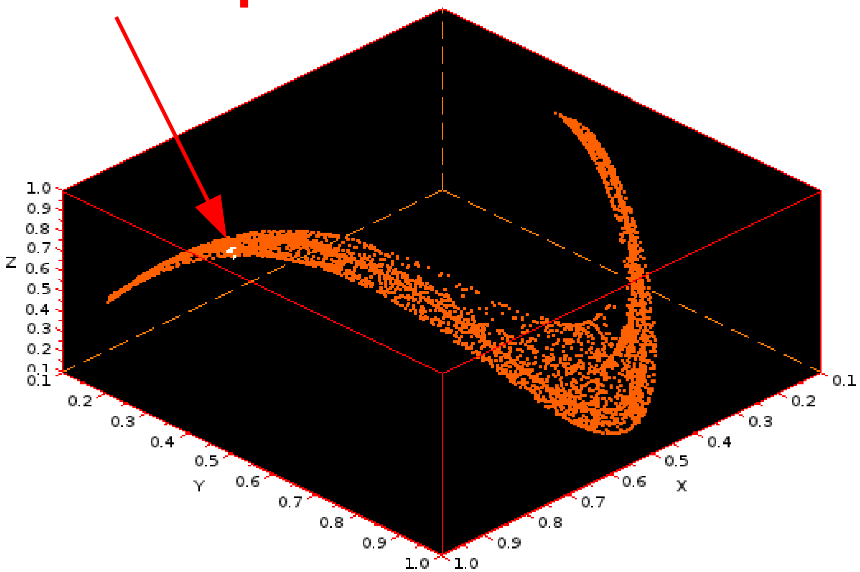

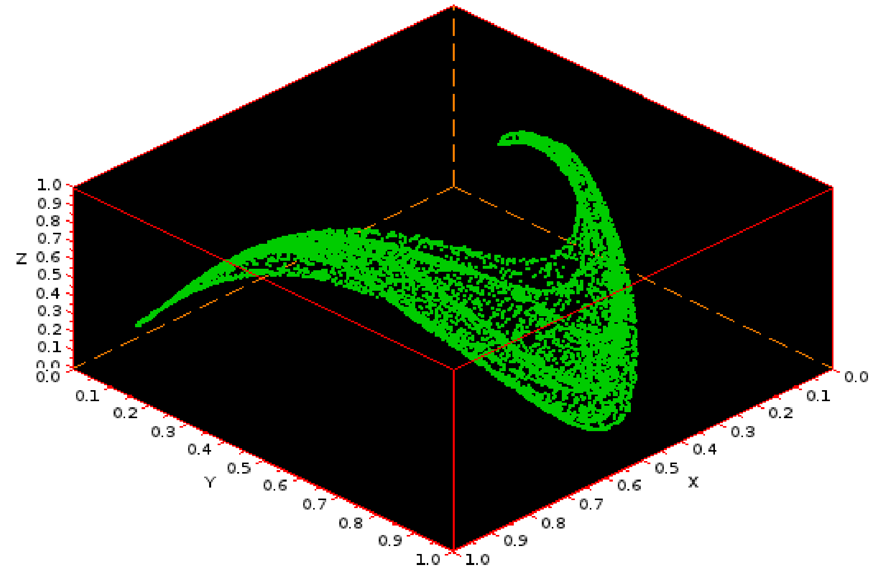

Reconstructed state-space from the
first data series in 3 embedding dimension

Reconstructed state-space from the
second data series in 3 embedding dimension

Both dataset formed a 2D manifold in the 3D embedding space

Sugihara's method: Convergent Cross mapping

Find its neighborhood!

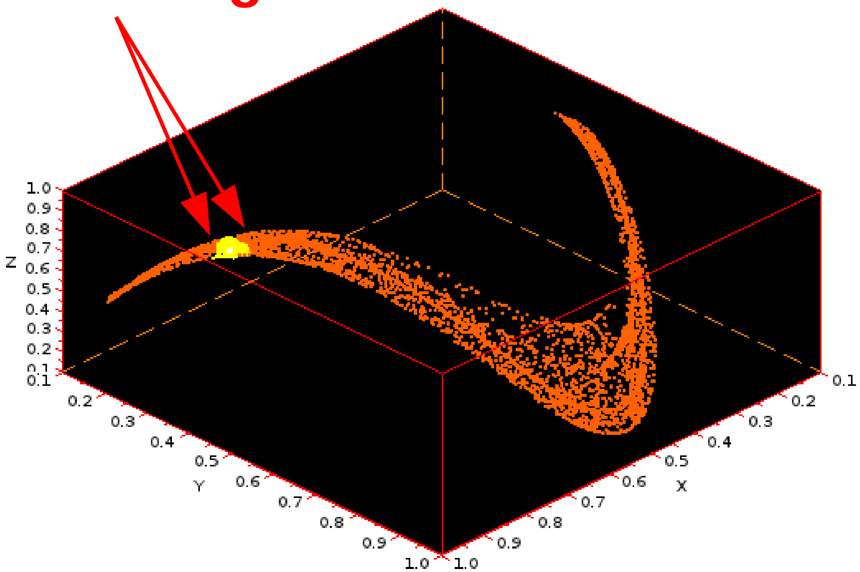

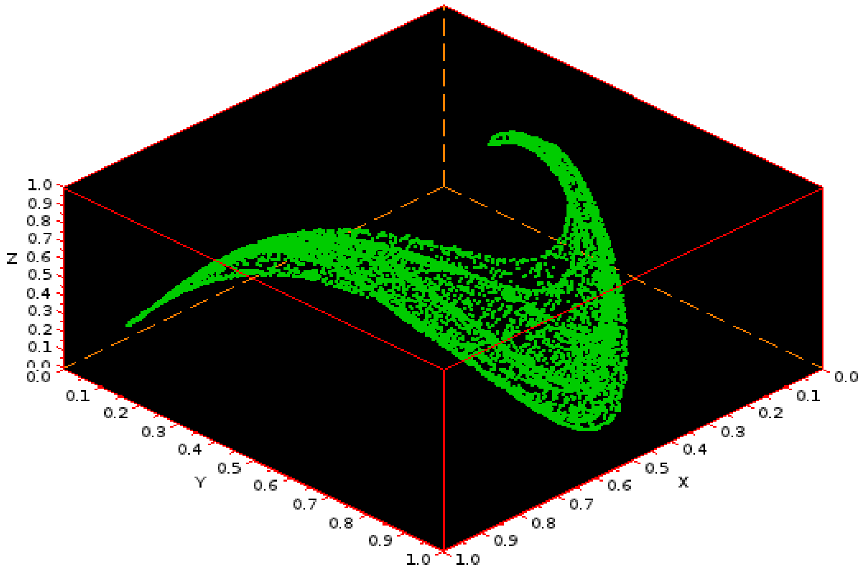

Reconstructed state-space from the first data series in 3 embedding dimension

Reconstructed state-space from the second data series in 3 embedding dimension

Both dataset formed a 2D manifold in the 3D embedding space.

Sugihara's method: Convergent Cross mapping

The images of the neighbors remained close to each other and to the image of the original point

Find the same time points in the other state space

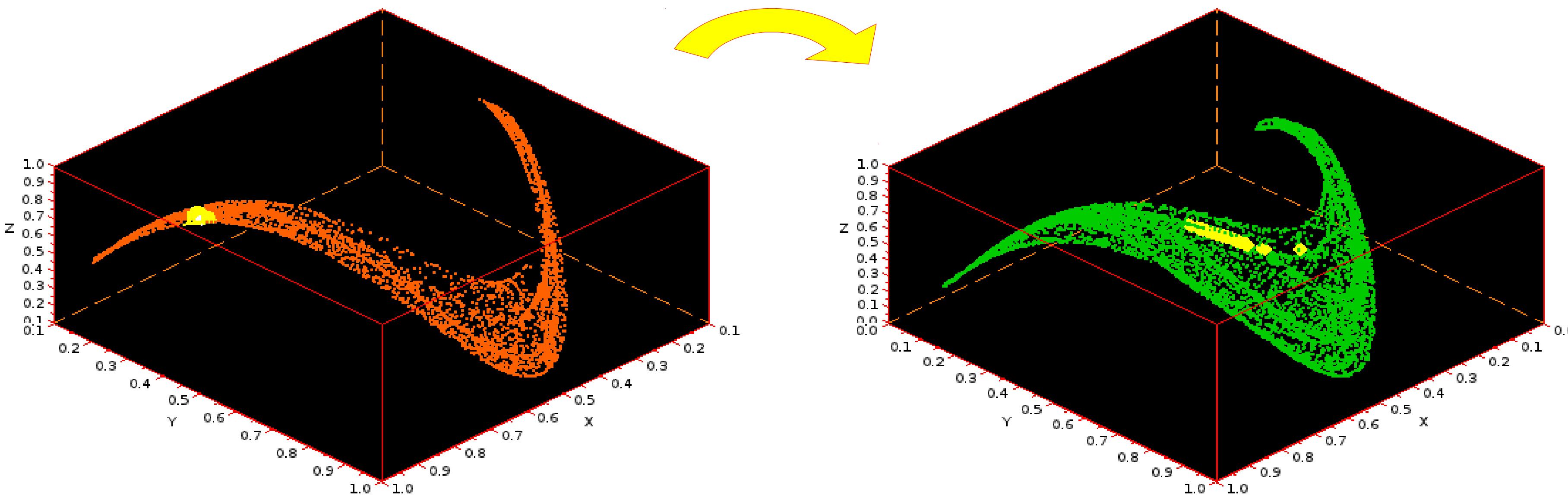

Reconstructed state-space from the first data series in 3 embedding dimension

Reconstructed state-space from the second data series in 3 embedding dimension

Lets do it for many points! If the neighbors in the first space are neighbors in the the second space as well, then the second variable is causal to the first one.

Sugihara's method: Convergent Cross mapping

In case of circular causality the mapping should work in both directions!

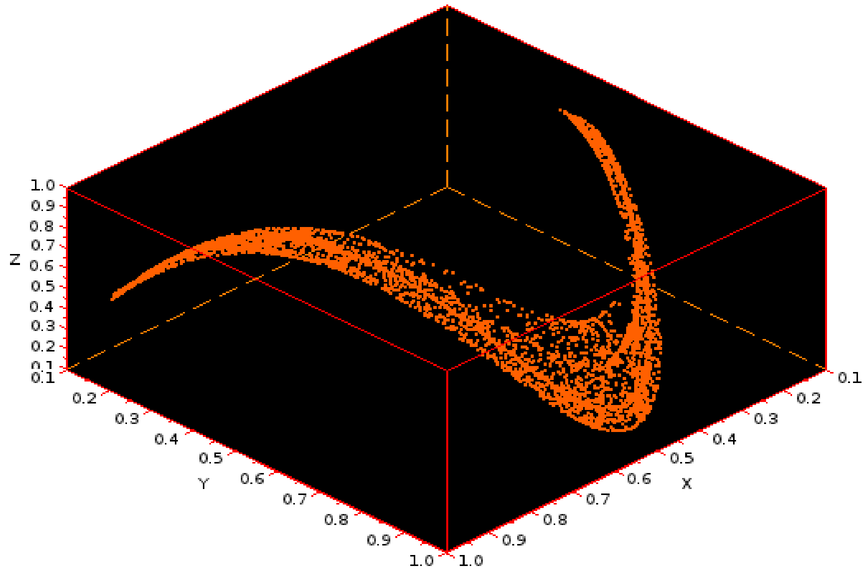

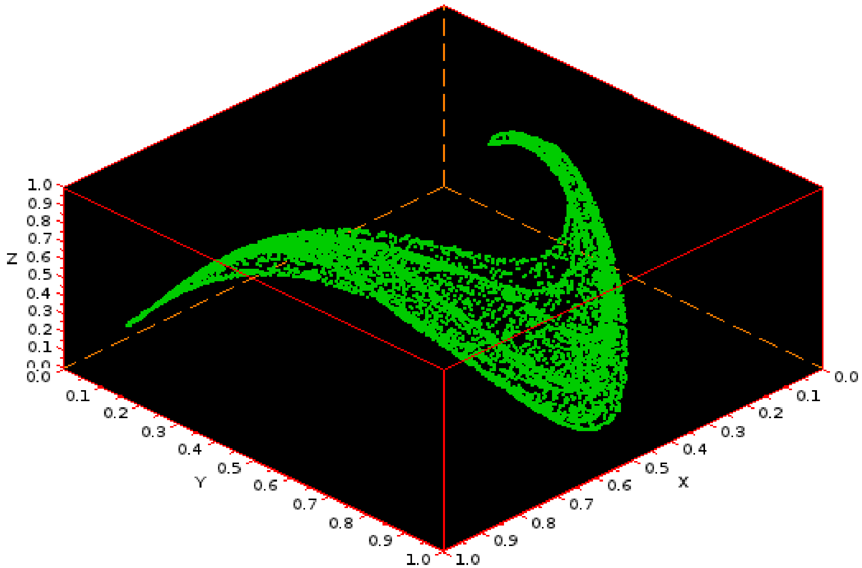

Reconstructed state-space from the first data series in 3 embedding dimension

Reconstructed state-space from the second data series in 3 embedding dimension

Let us do it into the other direction!

Sugihara's method: Convergent Cross mapping

Let us do it into the other direction!

The chosen point

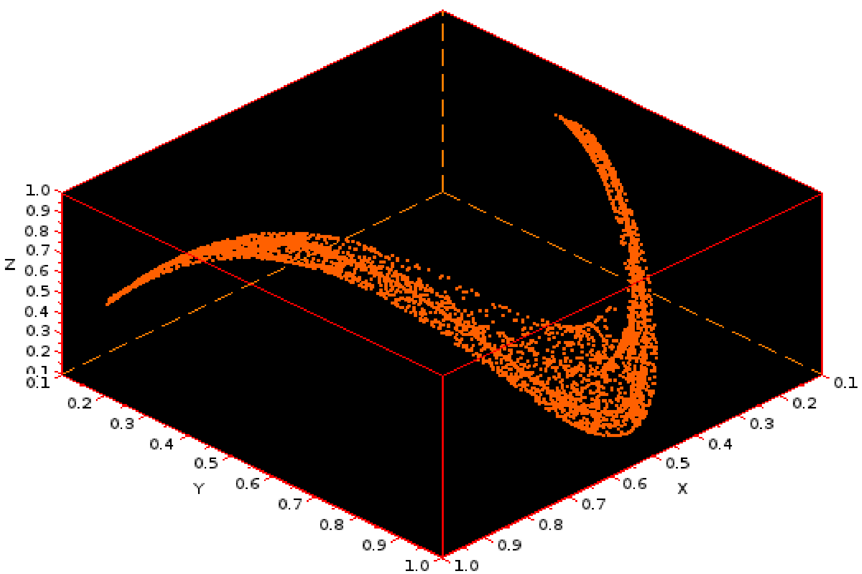

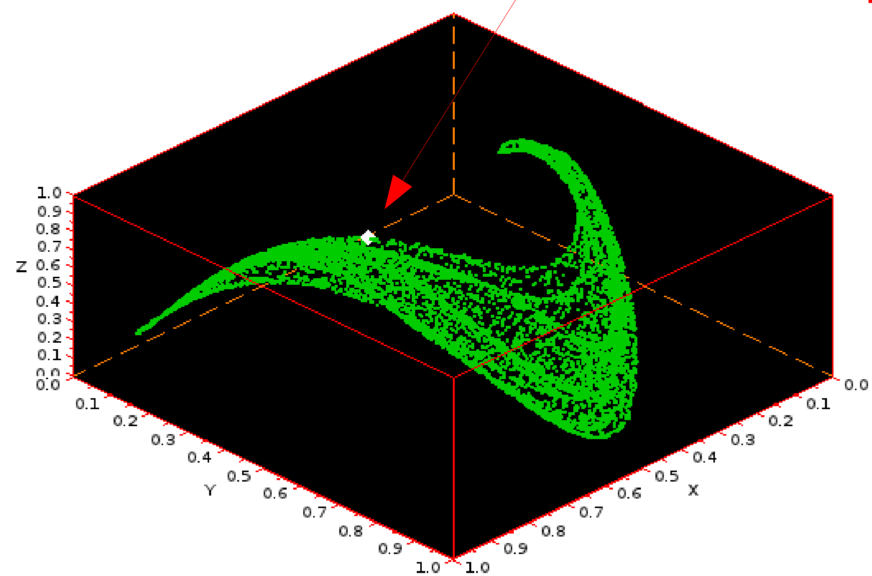

Reconstructed state-space from the
first data series in 3 embedding dimension

Reconstructed state-space from the
second data series in 3 embedding dimension

Sugihara's method: Convergent Cross mapping

Let us do it into the other direction!

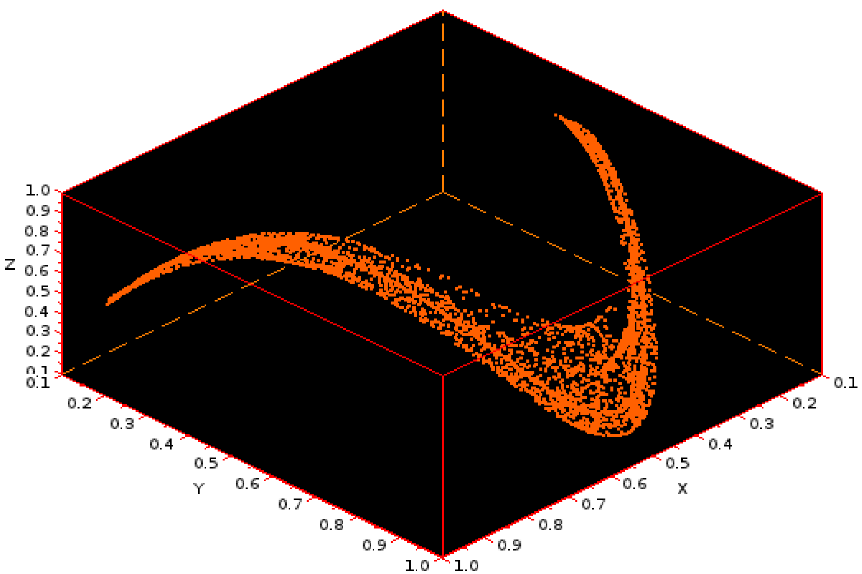

Reconstructed state-space from the first data series in 3 embedding dimension

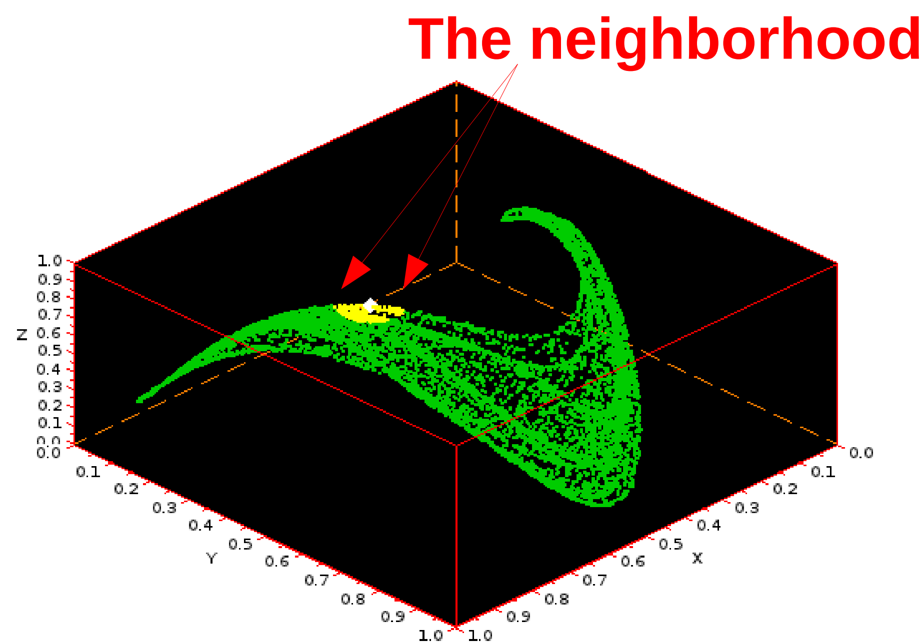

Reconstructed state-space from the second data series in 3 embedding dimension

Sugihara's method: Convergent Cross mapping

The mapping worked well into both directions!
This is the sign of circular causality.

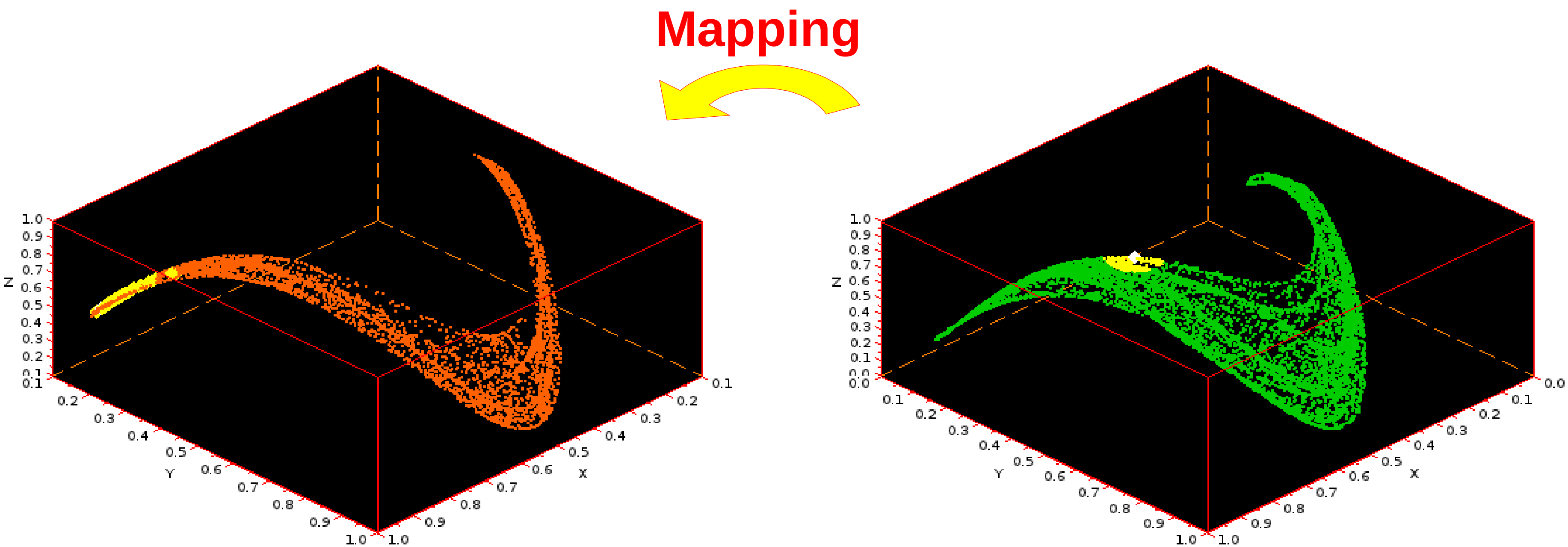

Reconstructed state-space from the first data series in 3 embedding dimension

Reconstructed state-space from the second data series in 3 embedding dimension

Cross mapping in case of unidirectional interactions

Case II.: Unidirectional, nonlinear coupling

$x_{n+1}=r_x x_n((1-x_n)+b_{yx}y_n)$

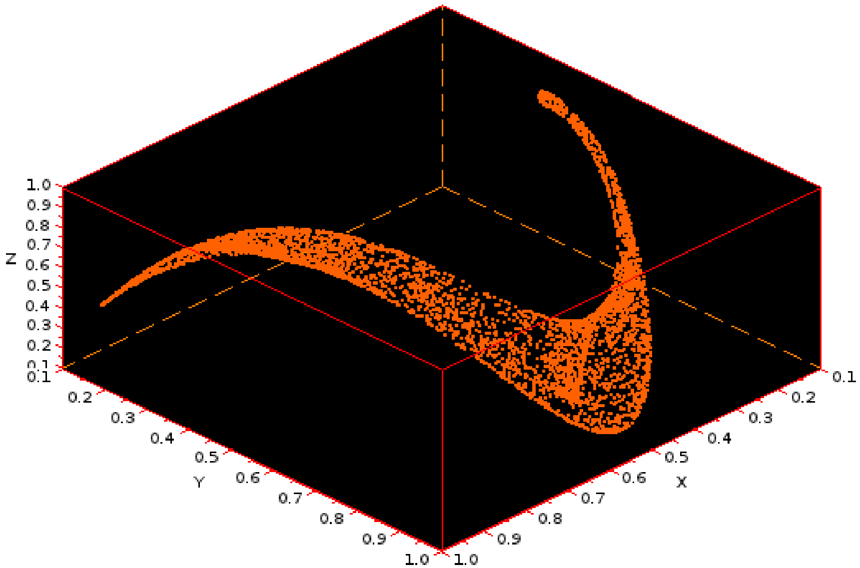

The consequence

$y_{n+1}=r_y y_n(1-y_n)$

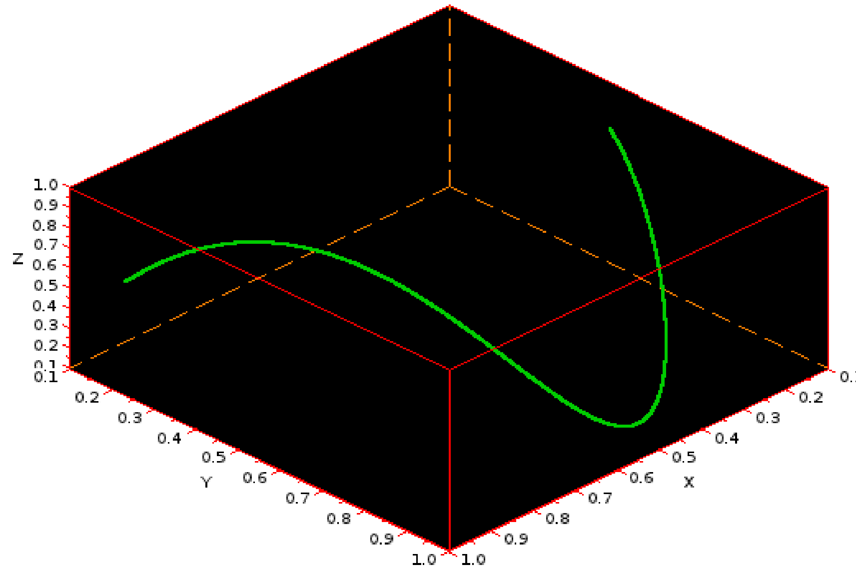

The cause

While the consequence formed a 2D manifold, the cause resulted an only 1D manifold in the 3D embedding space!

Cross mapping in case of unidirectional interactions

Mapping works well from consequence to cause

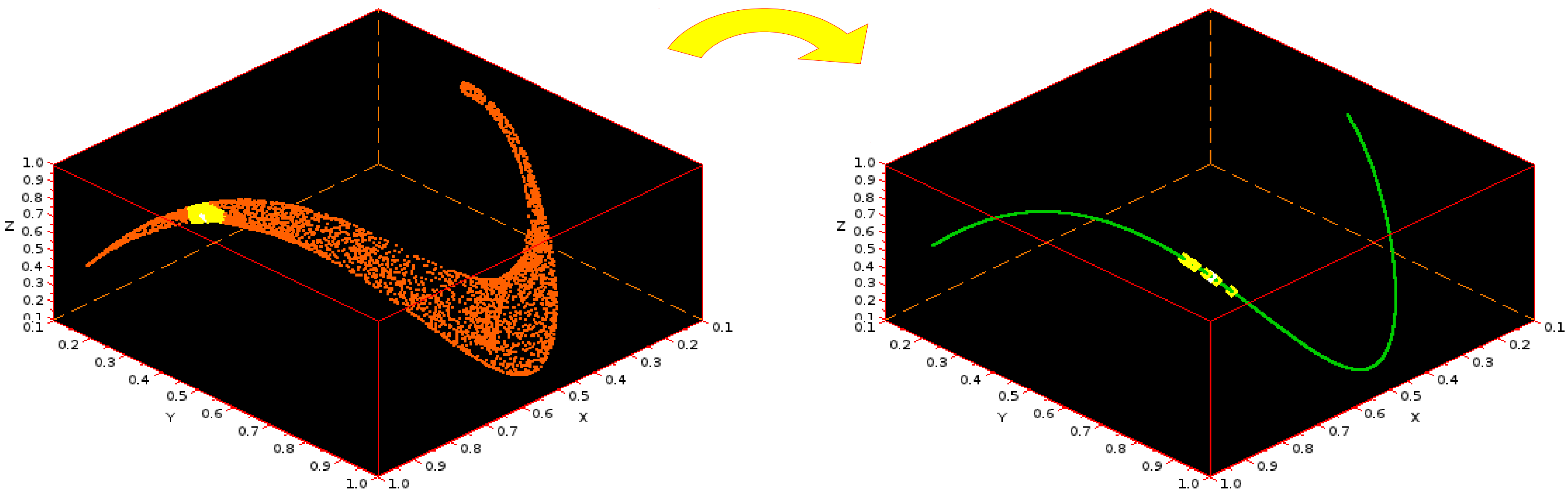

The consequence

The cause

While the first dataset formed a 2D manifold, the second dataset resulted an only 1D manifold in the 3D embedding space!

Cross mapping in case of unidirectional interactions

But spread out in the other direction!

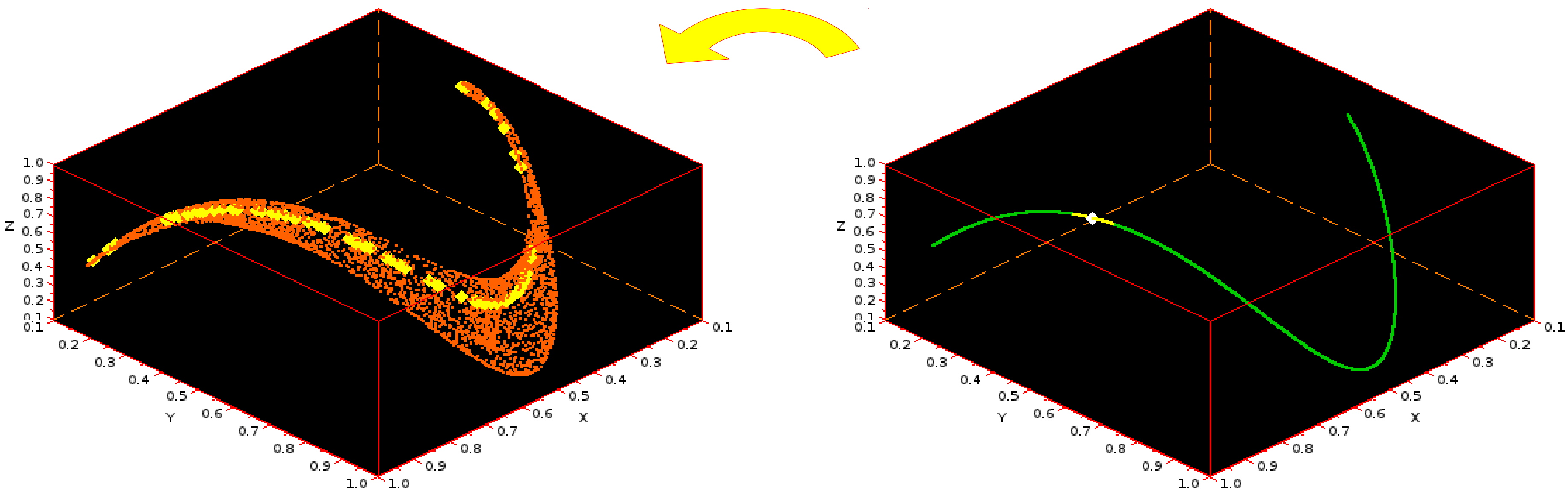

The consequence **The cause**

The mapping worked well from x to y but failed from y to x, showing, that y is causal to x but x is not causal to y.

Delayed cross map function

We have extended Sugihara's method for time-dependent and delayed connections. The method was tested on simulated coupled dynamical systems. Peaks positions on the negative axis mark the correct delay times.

Dorottya Cserpán

Zsigmond Benkő

Case I: Unidirectional coupling

The method precisely: identified the direction and the delay of the coupling: **X→Y**

Delay: 0

Delay: 0

Chaotic oscillator

Exponetial Decay

$X(t+1)=3.8X(t)(1-X(t))$

$Y(t+1)=0.8Y(t)+F(X(t-\text{delay}))$

$F(X)=e^{(1-X)^{10}}$ Non-linear coupling

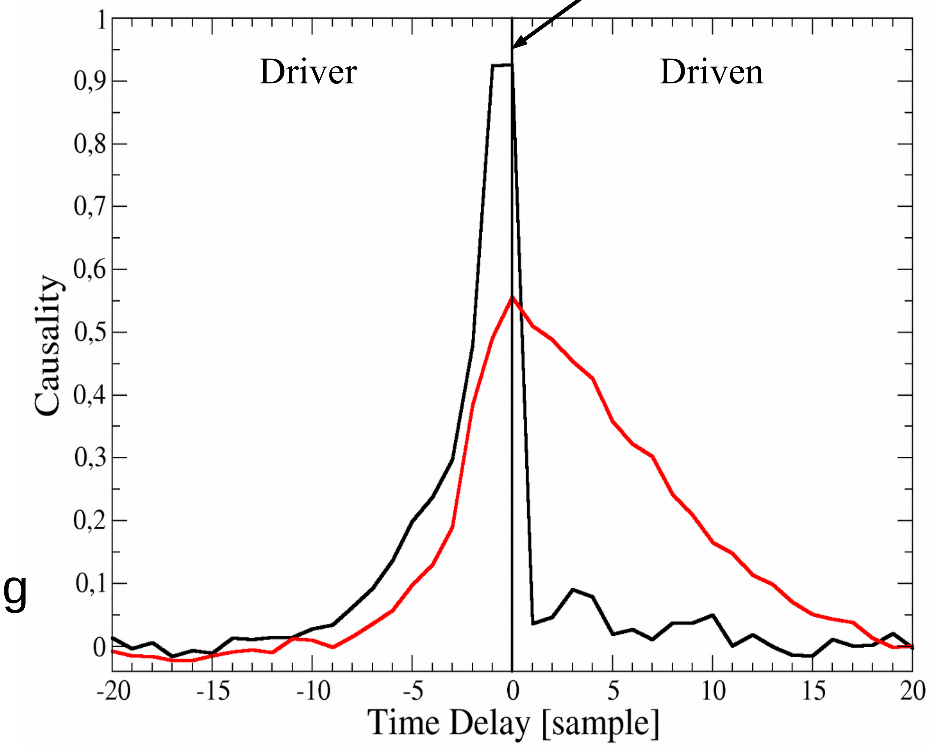

Delayed cross map function

The peak of the cross map functions follows precisely the delay of the effect

Case I:
Unidirectional coupling

Delay: 5

Chaotic oscillator

Exponetial Decay

$X(t+1)=3.8X(t)(1-X(t))$

$Y(t+1)=0.8Y(t)+F(X(t-\text{delay}))$

$F(X)=e^{(1-X)^{10}}$ Non-linear coupling

X → Y
Delay: 5

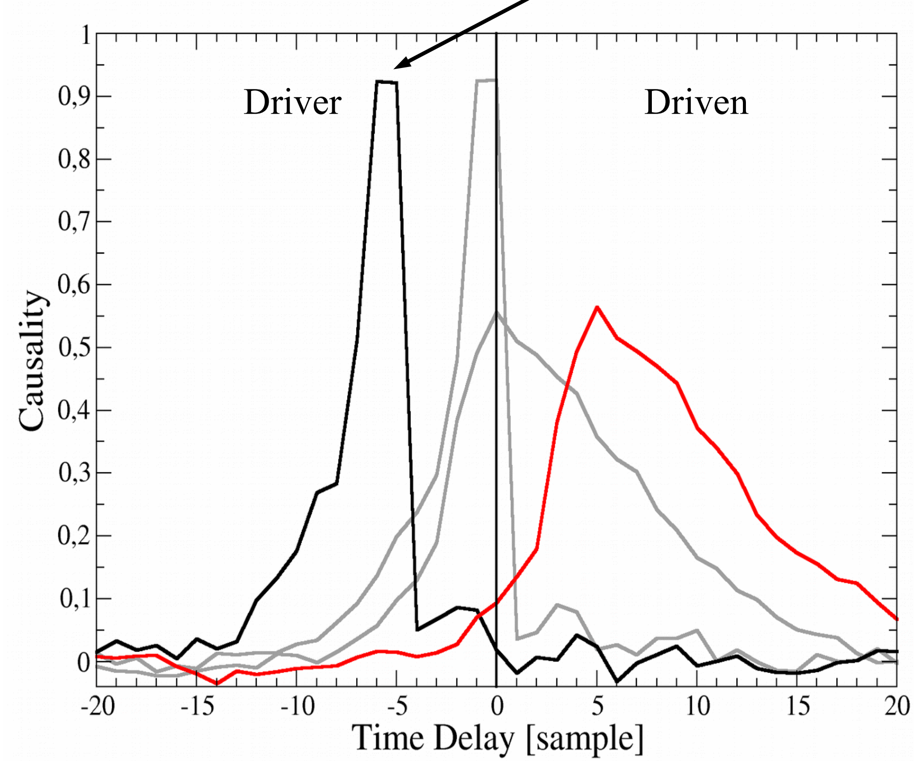

Delayed cross map function

The positive axis marks the anti-causal direction of the time shifts. This effect is stronger in deterministic systems and in case of strong couplings. In these cases, the future of the driven system can be predicted from the cause as well.

Case I:
Unidirectional coupling

Delay: 10

Chaotic oscillator

Exponetial Decay

$$X(t+1)=3.8X(t)(1-X(t))$$

$$Y(t+1)=0.8Y(t)+F(X(t-delay))$$

$F(X)=e^{(1-X)^{10}}$ Non-linear coupling

X → Y
Delay: 10

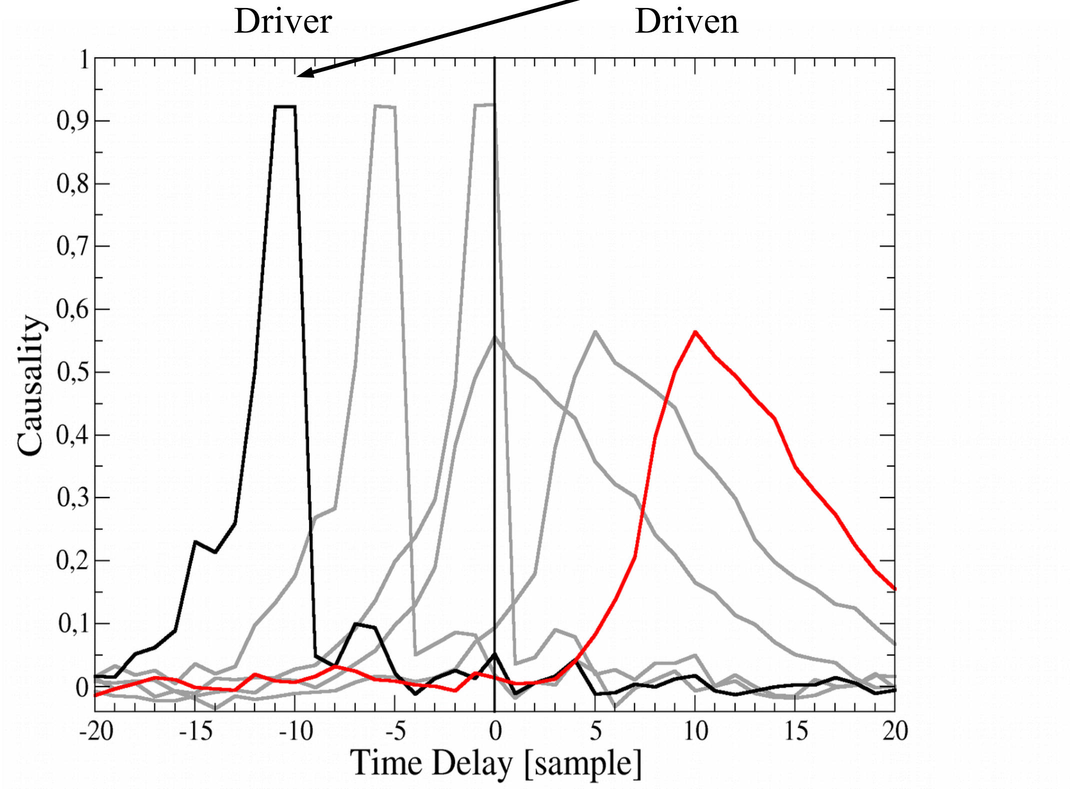

Delayed cross map function

In case of bidirectional coupling, the peak positions mark the correct delay times in both directions. The coupling coefficients could be different, and the delays could be the same or different into the two directions.

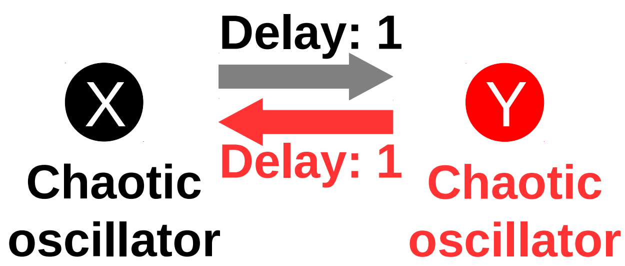

X(t+1)=3.8X(t)(1-X(t)+Y(t-delay))

Y(t+1)=3.8Y(t)(1-Y(t)+X(t-delay))

Non-linear coupling

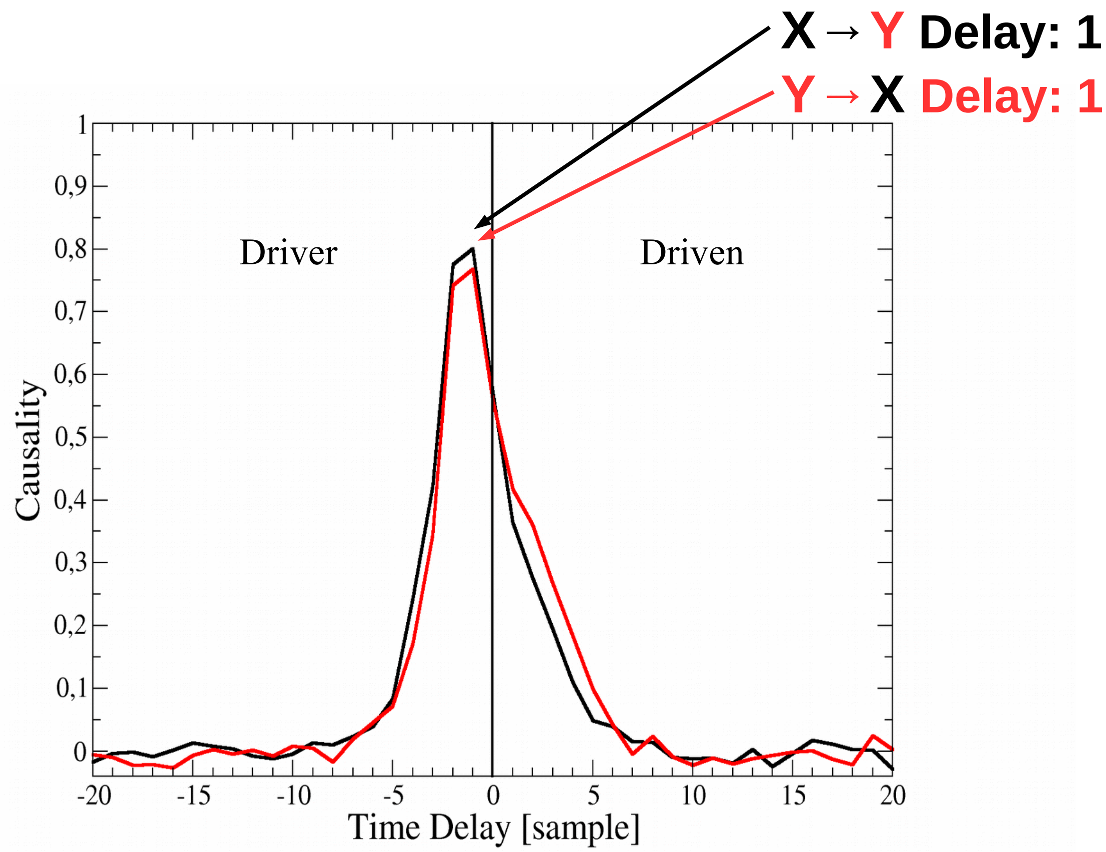

Delayed cross map function

In case of bidirectional coupling, the peak positions mark the correct delay times in both directions. The coupling coefficients could be different, and the delays could be the same or different into the two directions.

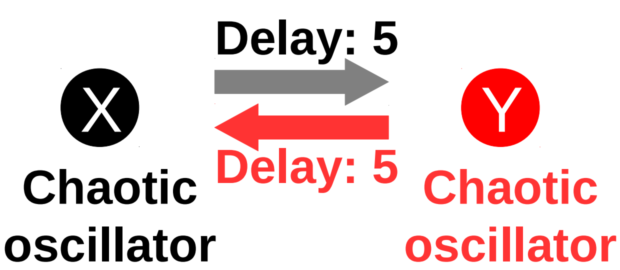

X(t+1)=3.8X(t)(1-X(t)+Y(t-delay))

Y(t+1)=3.8Y(t)(1-Y(t)+X(t-delay))

Non-linear coupling

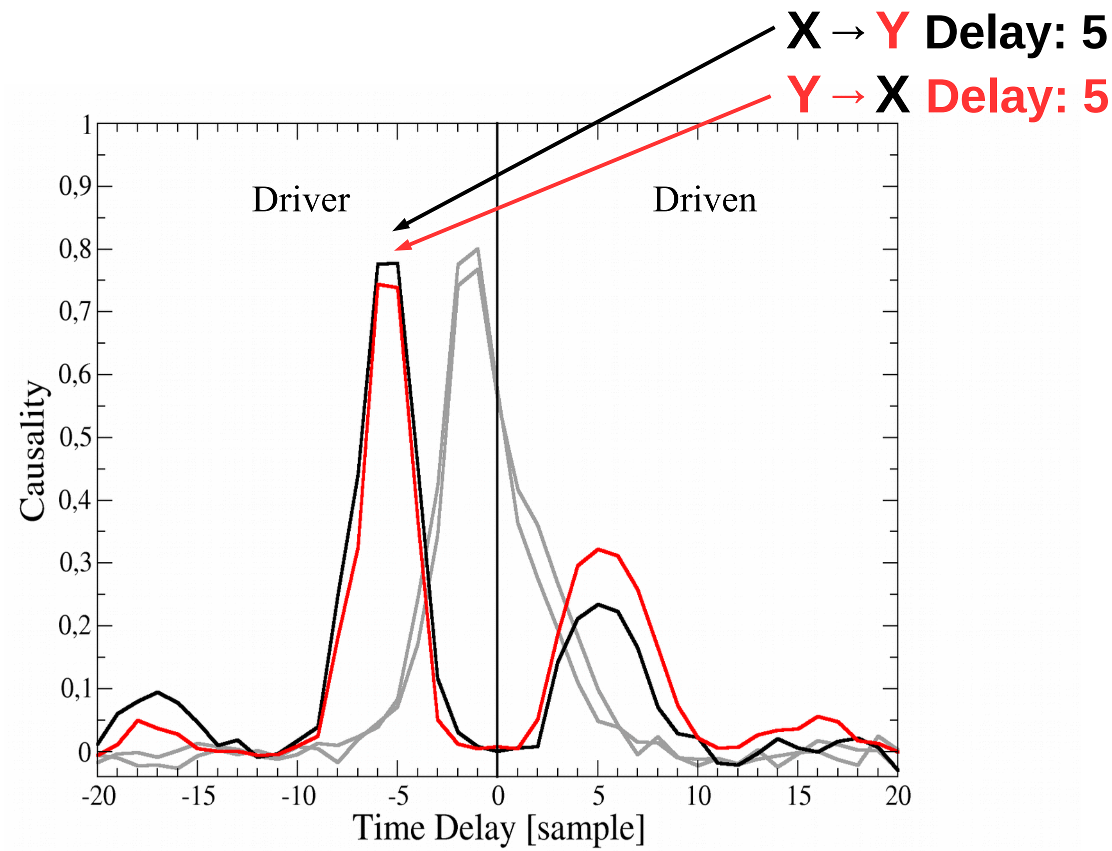

Delayed cross map function

In case of bidirectional coupling, the peak positions mark the correct delay times in both directions. The coupling coefficients could be different, and the delays could be the same or different into the two directions.

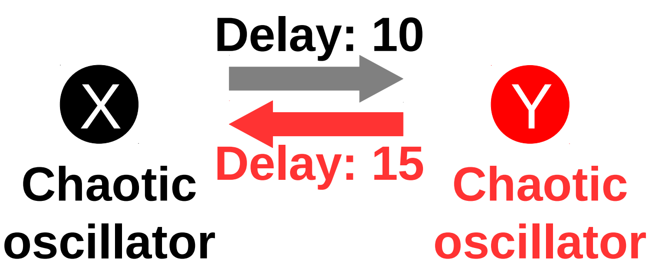

$$X(t+1)=3.8X(t)(1-X(t)+Y(t-delay))$$

$$Y(t+1)=3.8Y(t)(1-Y(t)+X(t-delay))$$

Non-linear coupling

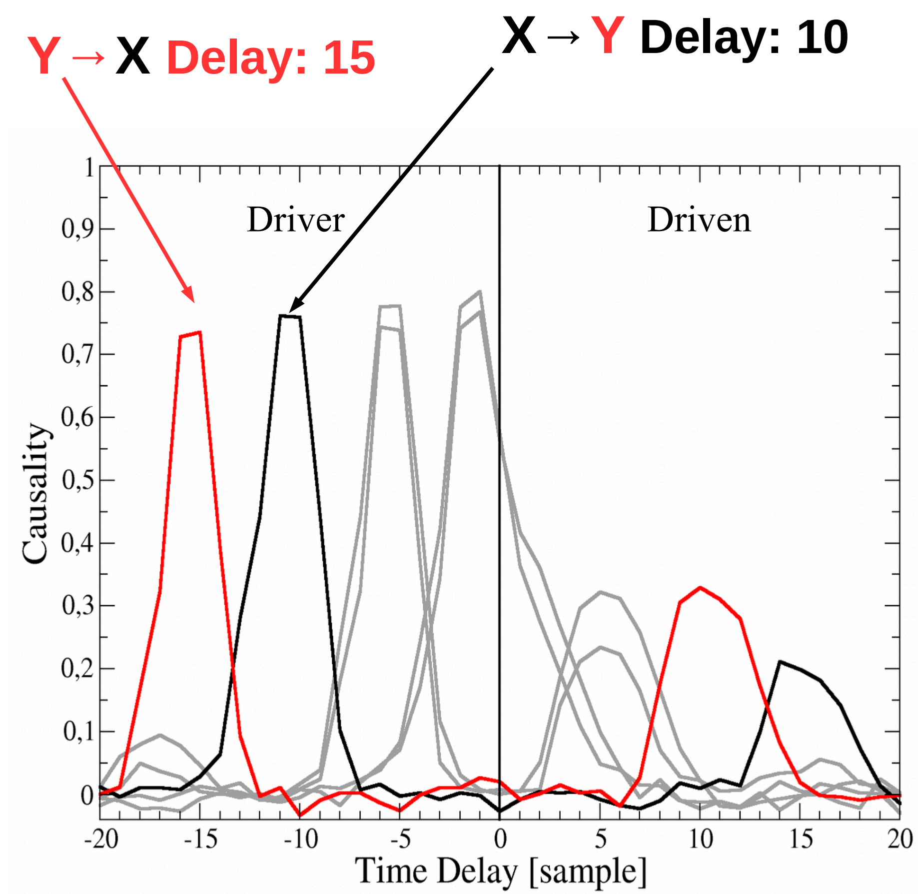

LFP vs IOS

Epileptiform activity was evoked by low Mg+ environment in vivo slice preparation. The local field potential was recorded together with the intrinsic optical signal (IOS), which is possibly a result of swelling of cells during over excitation.

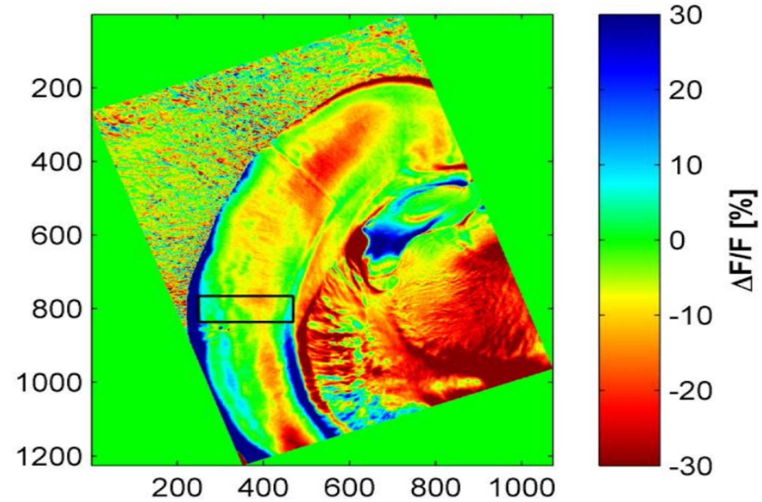

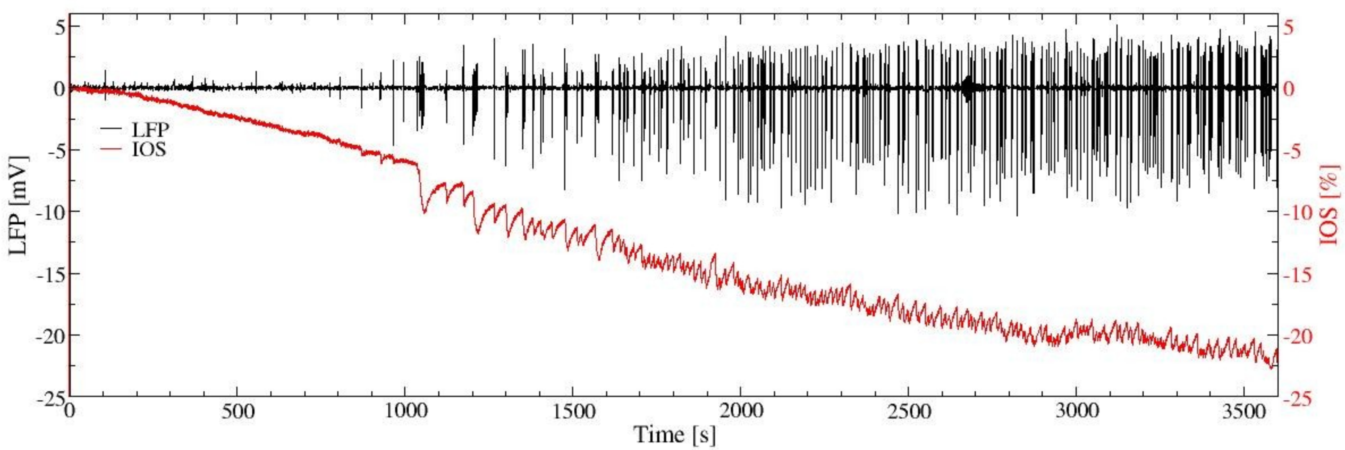

During the long (1 hour) recording, epileptiform bursts appeared with increasing frequency. Parallel, the optical reflectance (and the transmittance) of the tissue changes for visible light, without any additional dying. The process is clearly activity dependent, but slow.

Ildikó Világi

Sándor Borbély

Kinga Moldován

Eötvös Loránd University
Department of Physiology and Neurobiology

LFP vs IOS

The faster component were inverted comparing reflected and transmitted light, while the slow component was negative both cases.

Different mechanisms:

IOS low → absorbtion

IOS high → transmittance

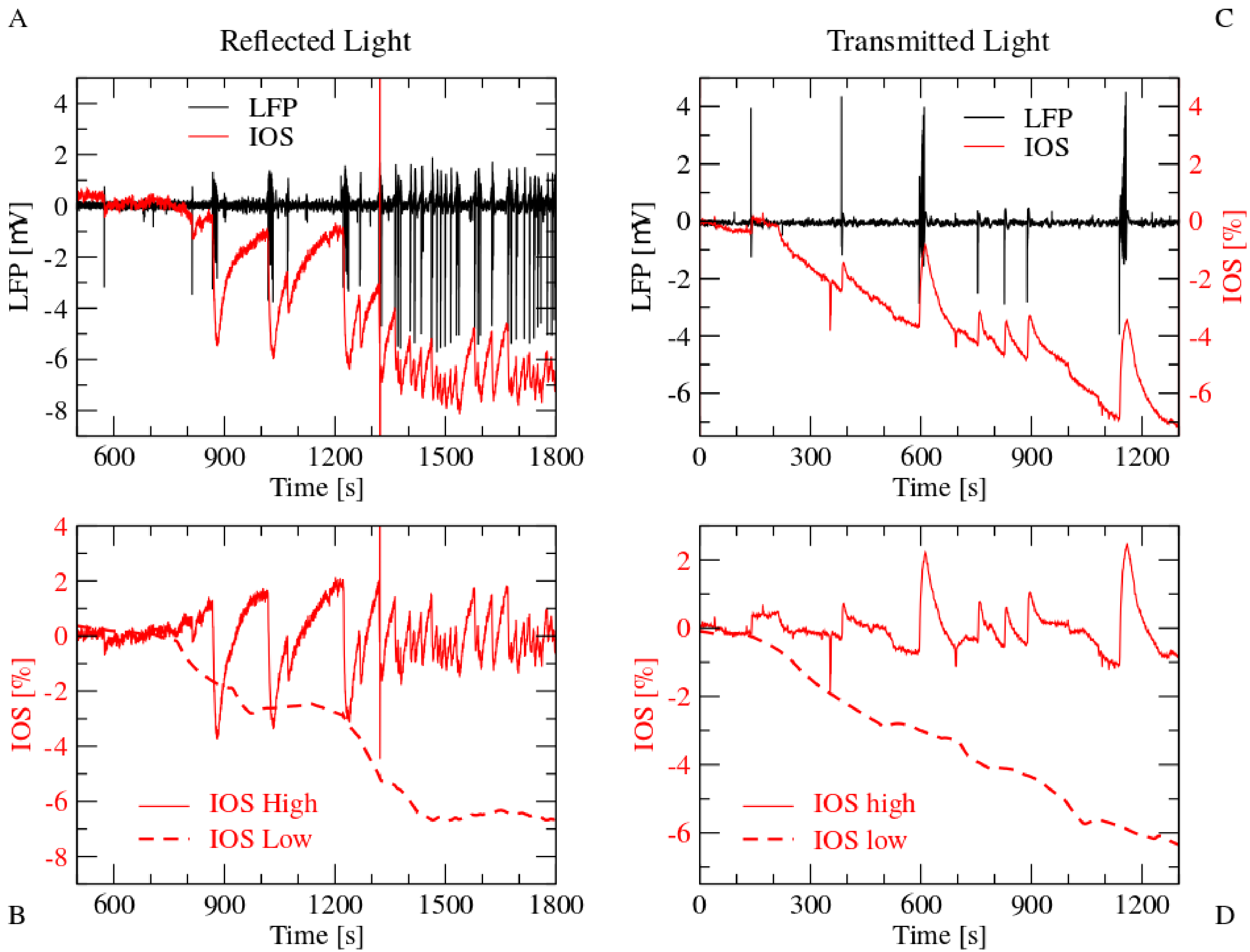

LFP vs IOS

The sampling frequency of the IOS was only 2Hz, much lower than the 1kHz of the LFP!!!

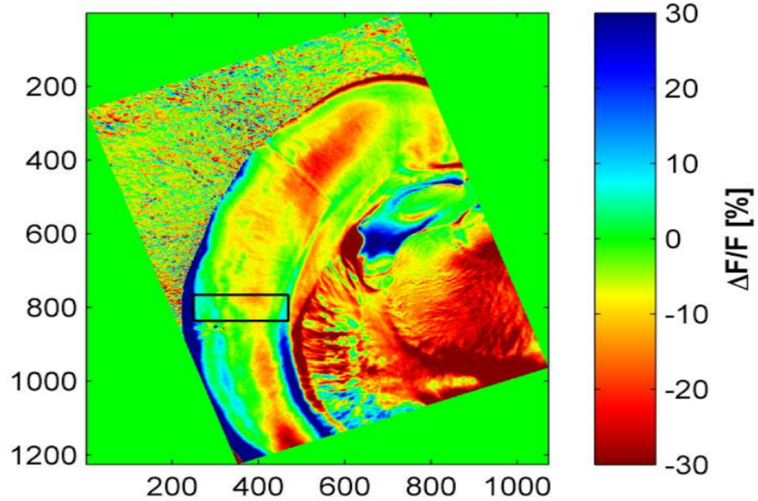

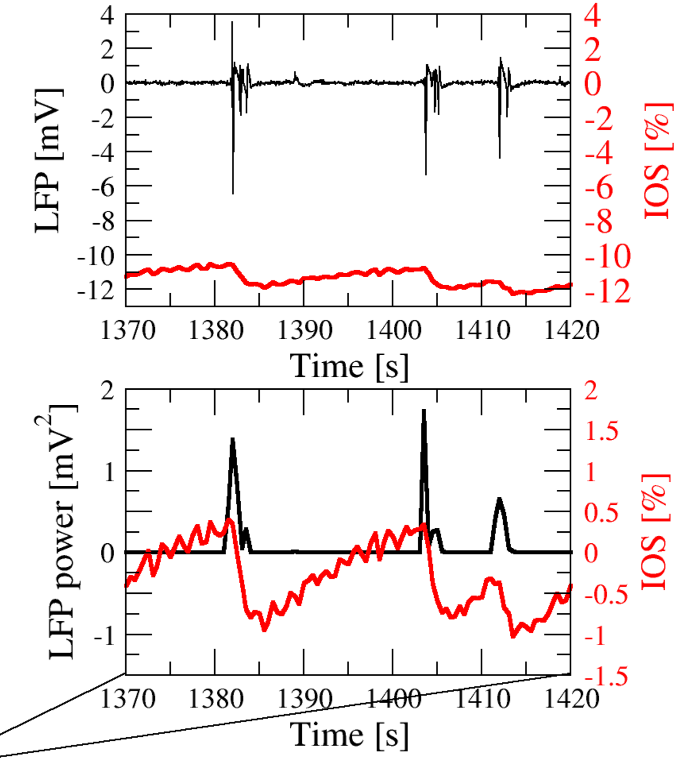

In order to make the causality analysis applicable:

The faster and slow component of the IOS were divided by subtracting a moving window average,to get stationary time series.

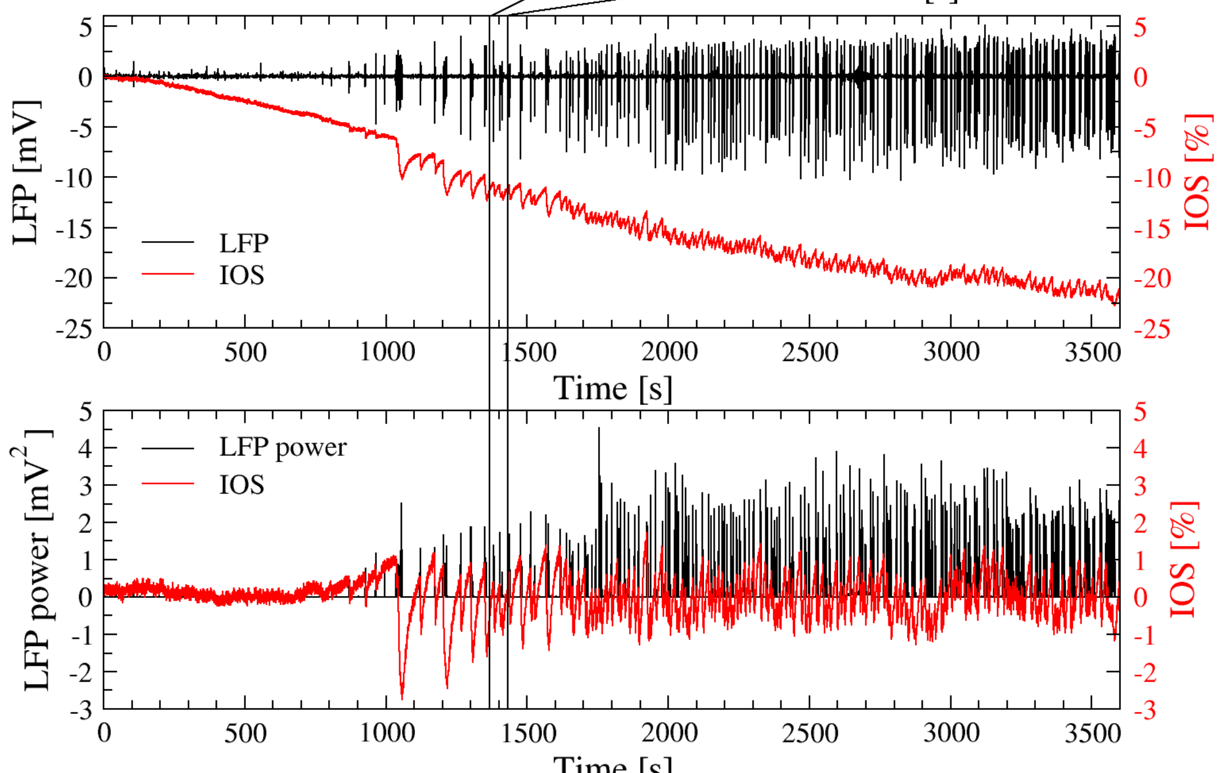

The LFP has been downsampled by summing up the V^2 for every 500 ms

LFP-IOS cross correlation

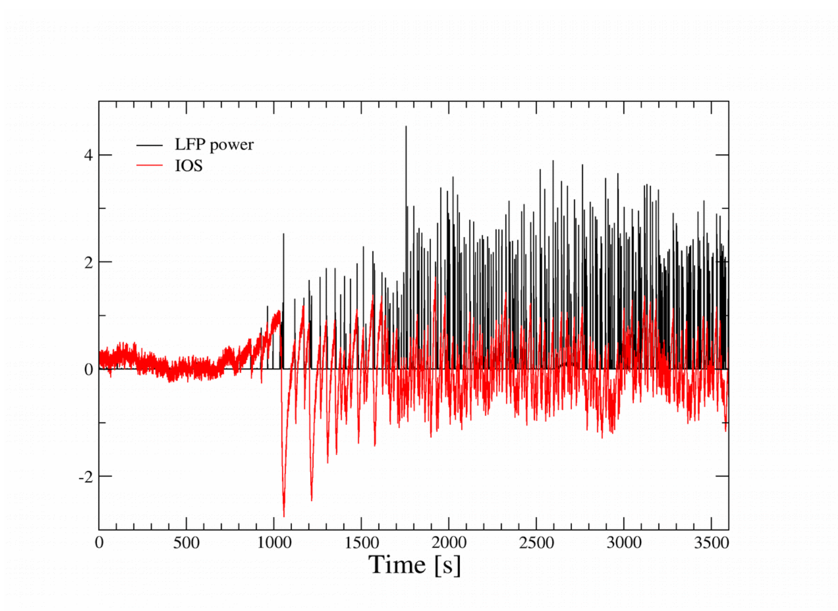

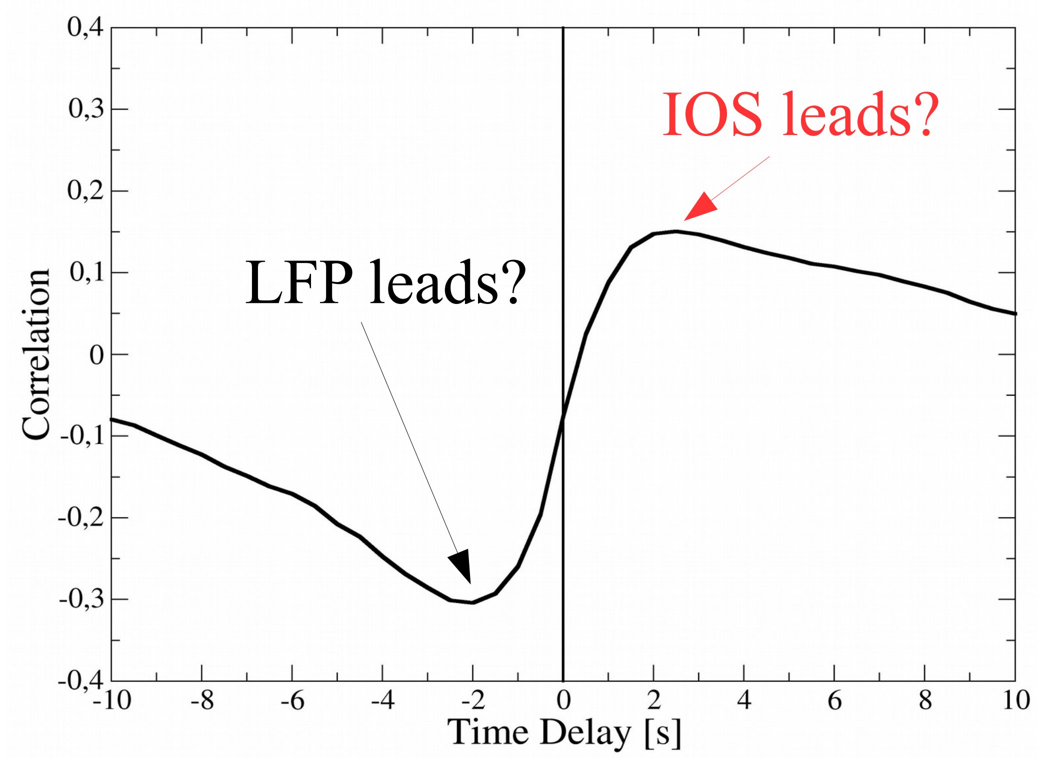

The instantaneous correlation is nearly zero, the cross correlation function has two significant peaks: a higher negative one at -2s (LFP leads) and a smaller positive one at +2.5s (IOS leads). This could be the sign of a well delayed interaction.

Delayed cross map function

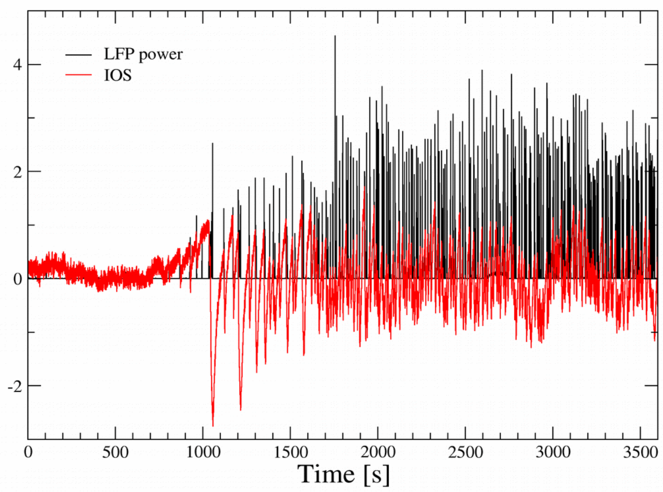

LFP → IOS Delay: 500 ms

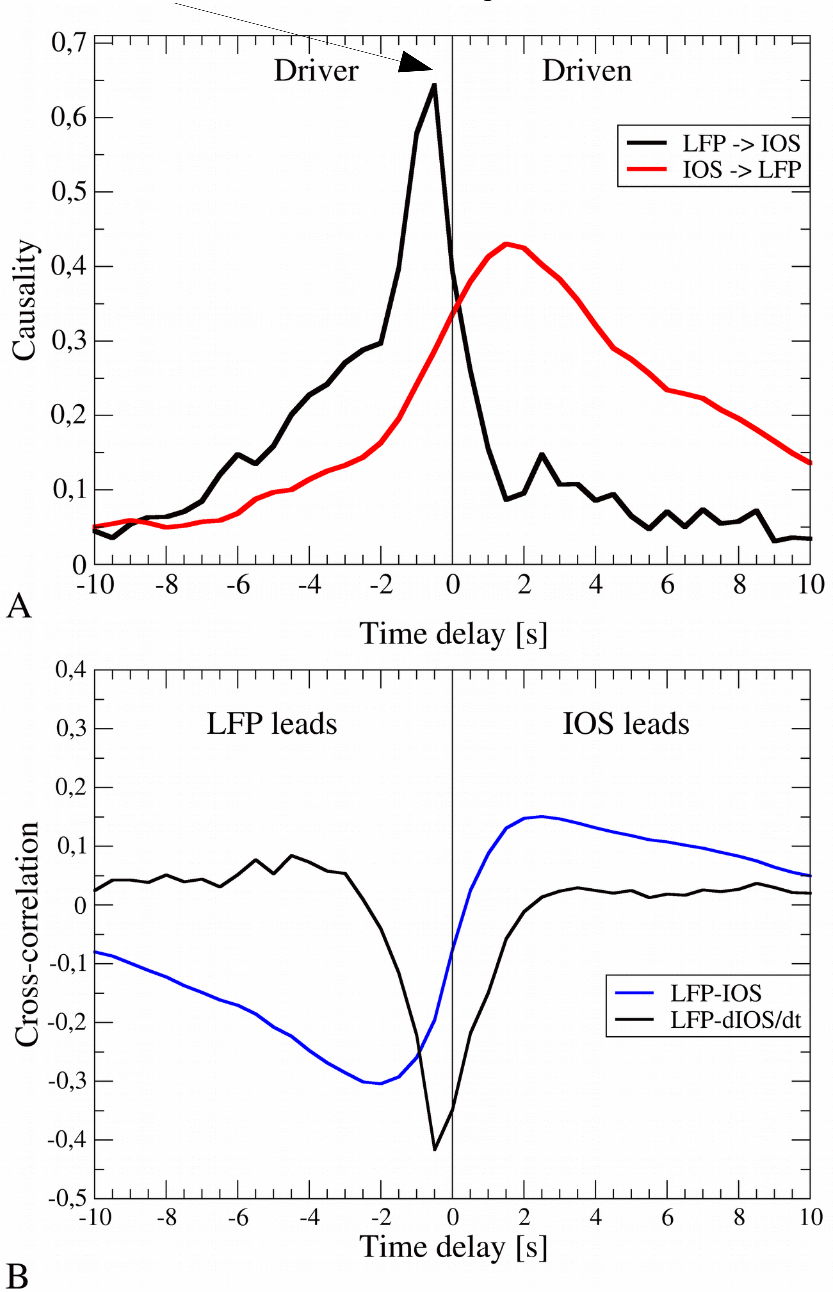

Instead:
Delayed Cross Map function shows a causal effect from LFP to IOS with 500ms delay, corresponding to 1 sample time for IOS.
Although, the time scale of the two signals were very different, the unidirectional causal effect was revealed.

Delayed cross map function

The causal relationship was significant and independent from the form of evoking the epileptic activity.

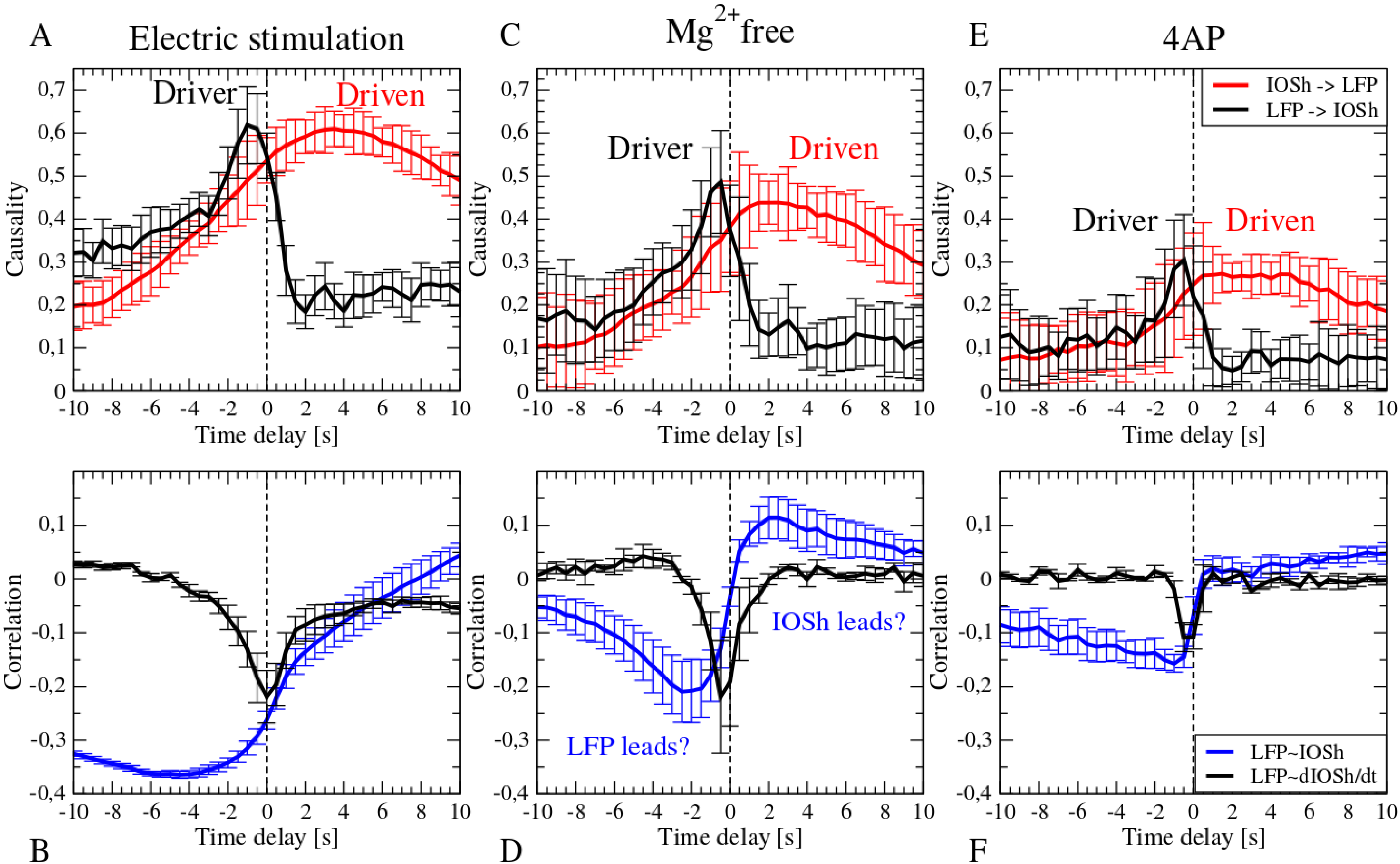

Time evolution of the coupling

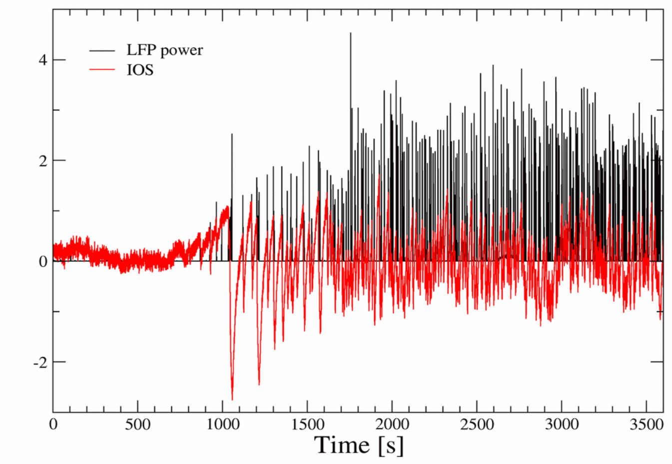

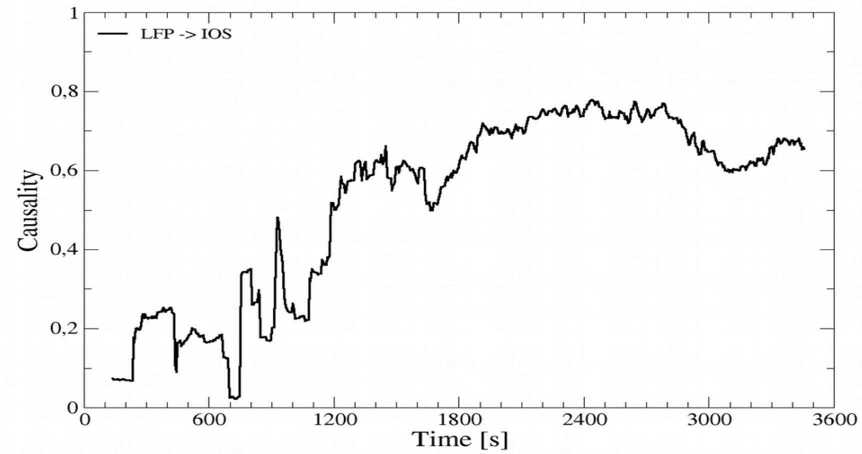

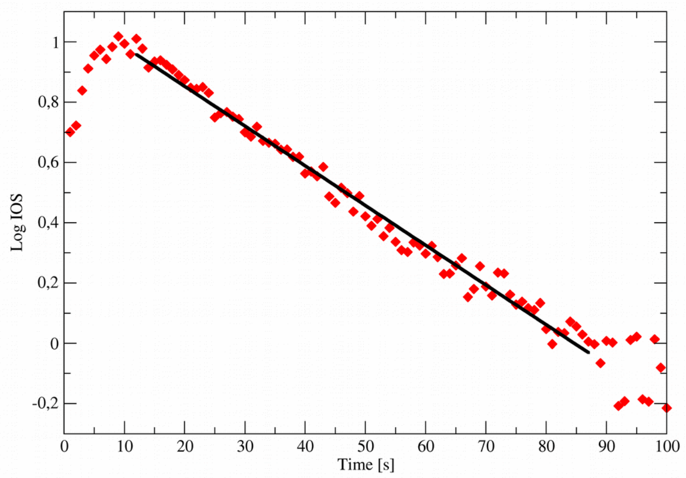

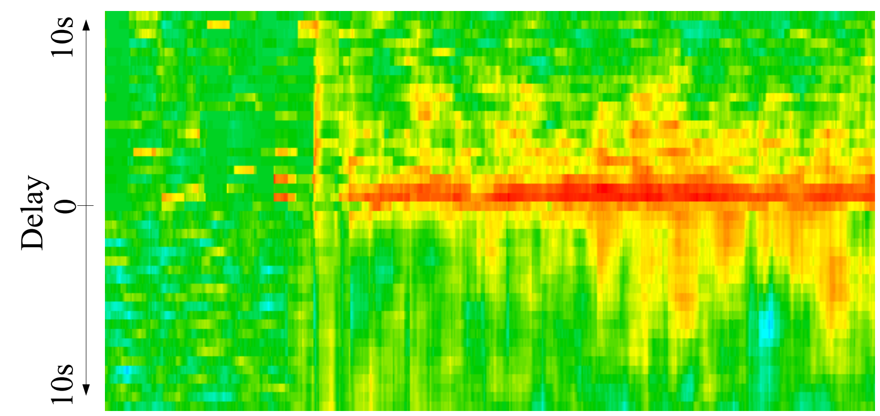

Between epileptic bursts, IOS decay exponentially

Strength of causality increased with the increasing frequency of the epileptic bursts

Reverse engineering

$$\frac{dIOSh}{dt} = W(t) * LFP^2 - \frac{IOSh(t)}{\tau_{high}}$$

Where:

$$W(t) = W_0 * e^{\frac{-t}{\tau_{low}}}$$

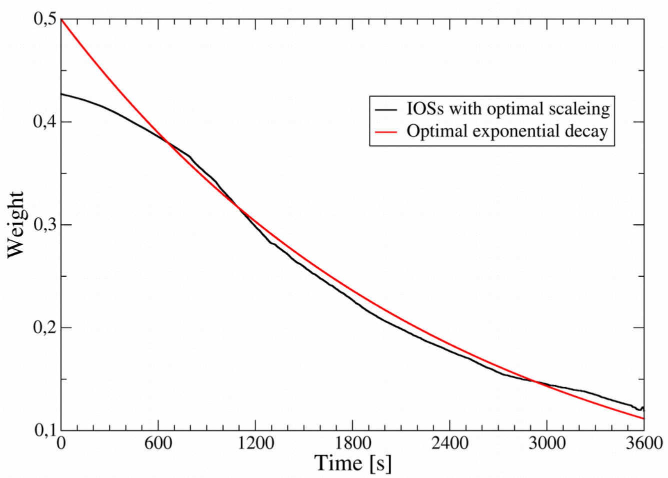

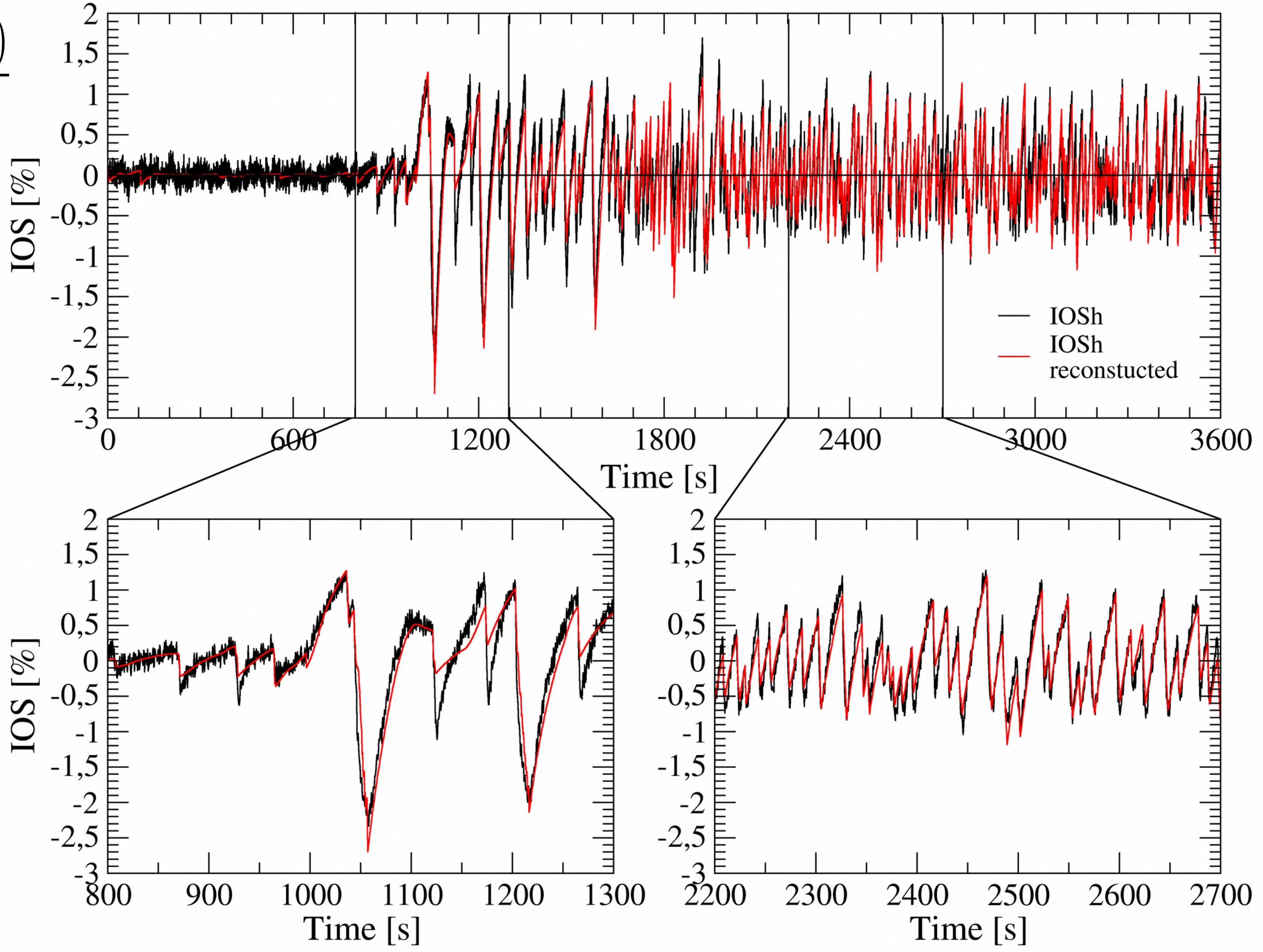

The IOS time series was reconstructed, based on the LFP recording with high precision during the 1h long session.

Reverse engineering

$$\frac{dIOSh}{dt}=W(t)*LFP^2-\frac{IOSh(t)}{\tau_{high}}$$

Where:

$$W(t)=W_0*e^{\frac{-t}{\tau_{low}}}$$

The same model, with different parameters describes the 4AP activity as well.

4AP case

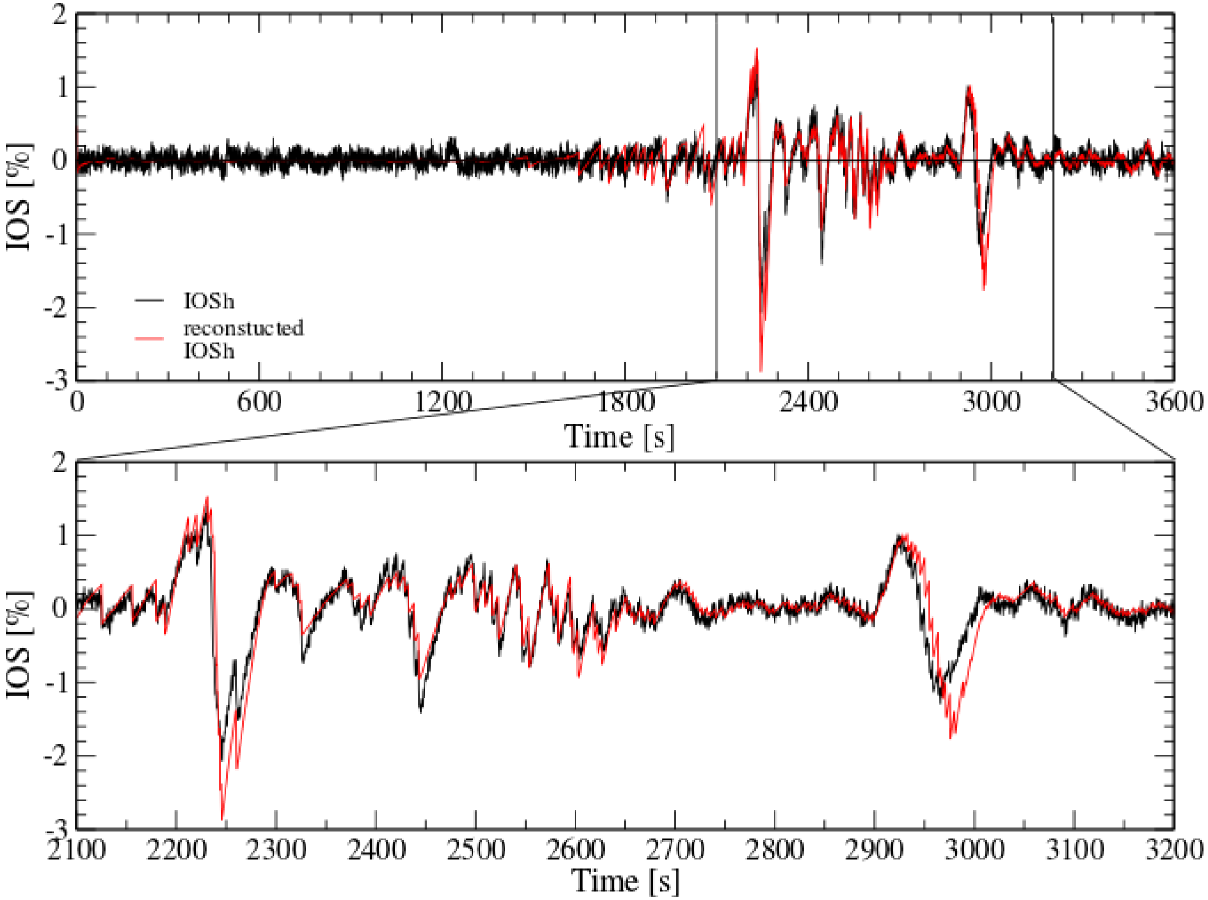

Intra- and inter hippocampal connectivity during seizure

In order to find out the lateralization of the seizure onset, two near-hippocampal electrodes inserted through the foramen ovale into the lateral ventricles.

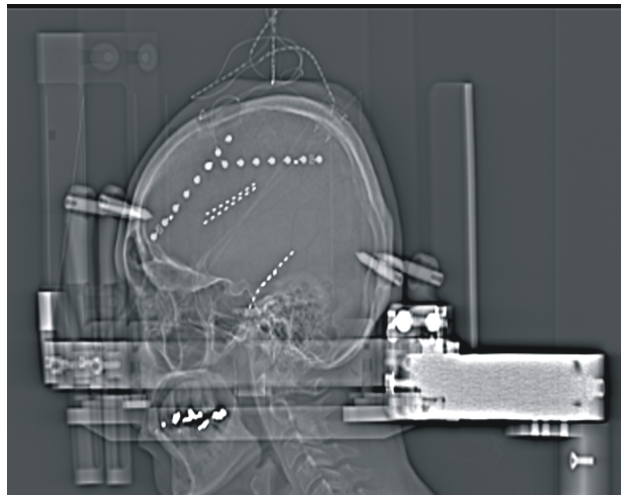

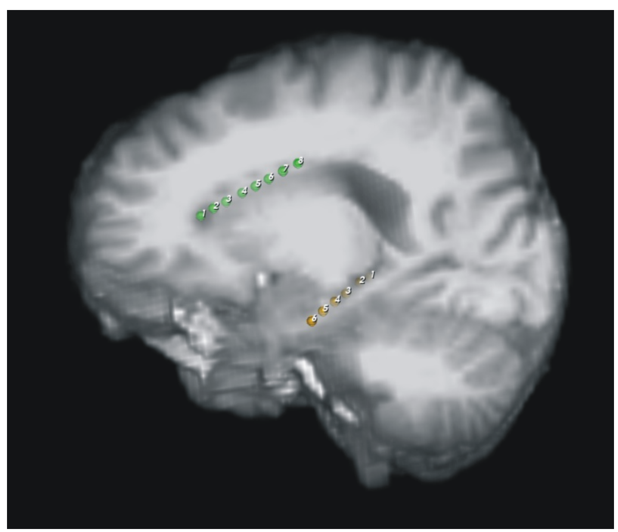

National Institute of Clinical Neurosiences

Péter Halász

Loránd Eröss

Dániel Fabó

László Entz

Boglárka Hajnal

Emilia Tóth

Márta Virág

Virág Bokodi

Intra- and inter hippocampal connectivity during seizure

From the 2*6 channel bilateral hippocampal potential recordings 2*4 channel CSD were calculated.

The causality analysis were applied to the temporal derivative of the CSD.

The connections which were active before the seizure stops, but new, more extended connection structure emerges during the seizure.

Causality

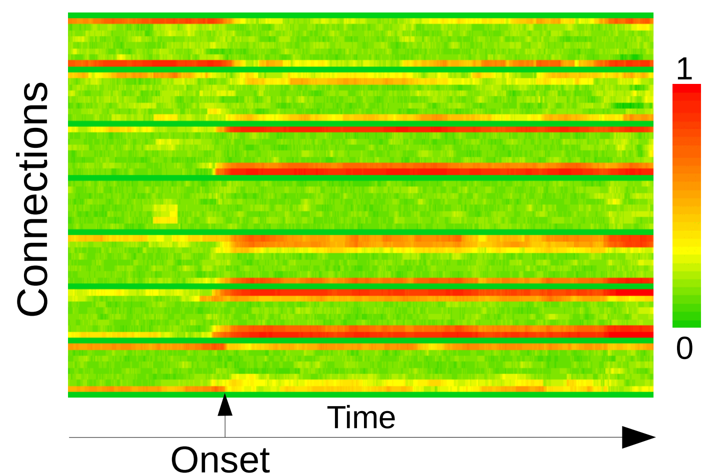

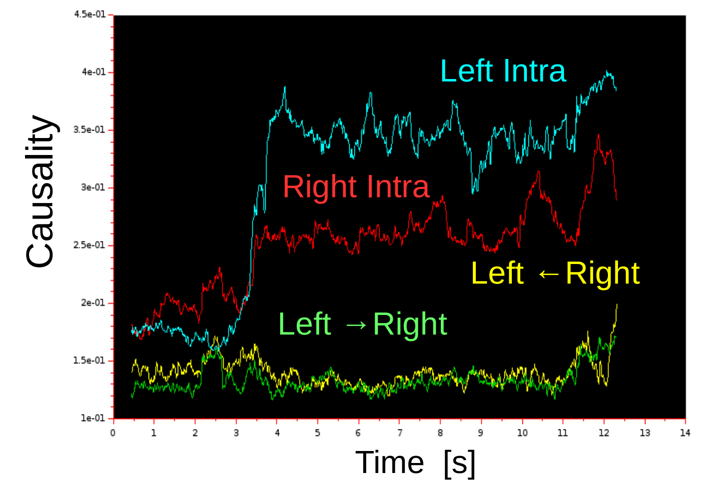

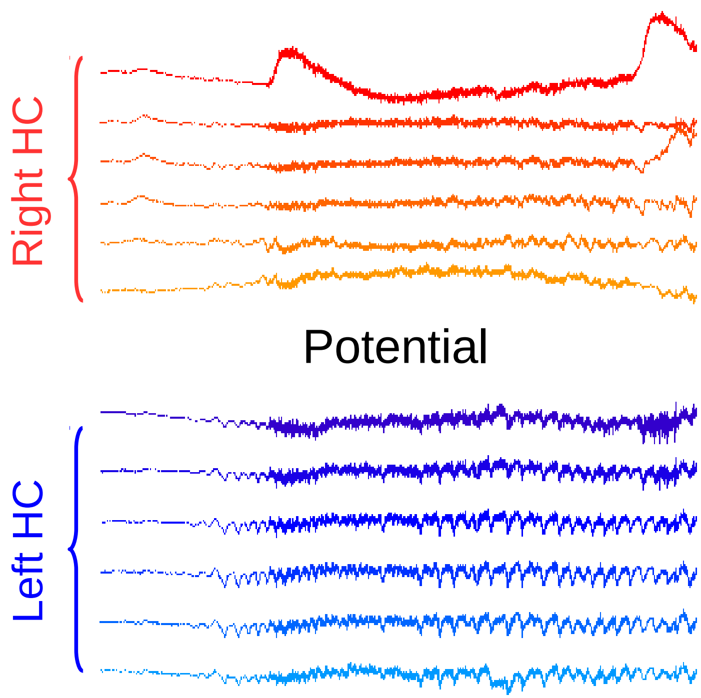

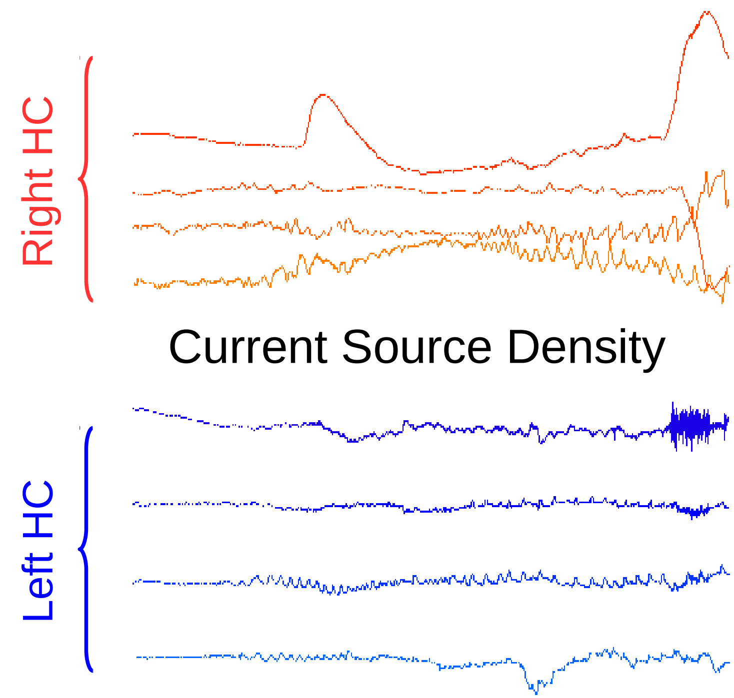

Intra- and inter hippocampal connectivity during seizure

During seizure, the intra-hippocampal connections emerged and spread out for larger distances, while the inter-hippocampal connections dropped down.

The connection structure before and during the seizure was very conservative through different seizures in this patient.

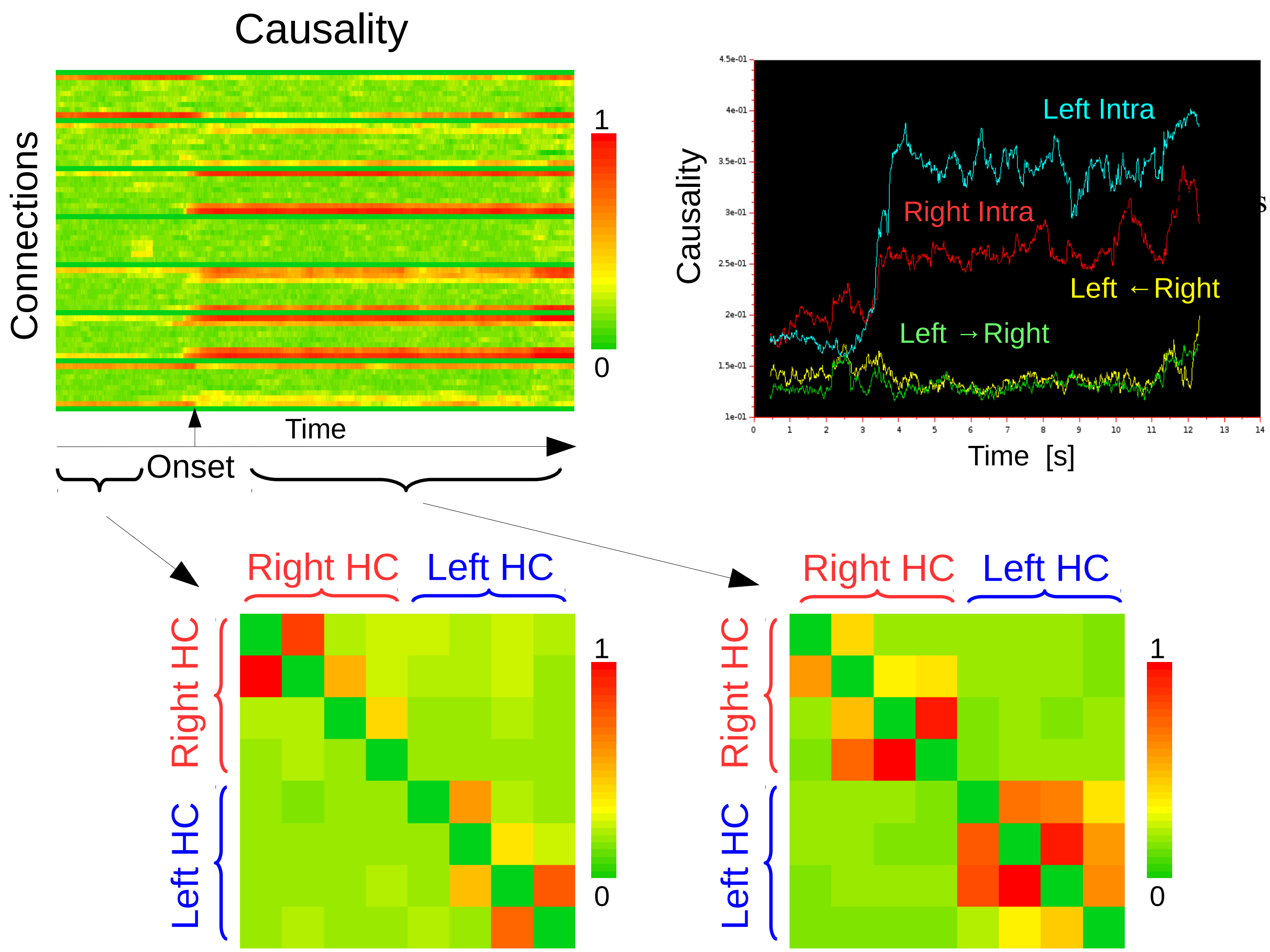

Connection matrices before and during seizure

Causality between the hippocampal layers

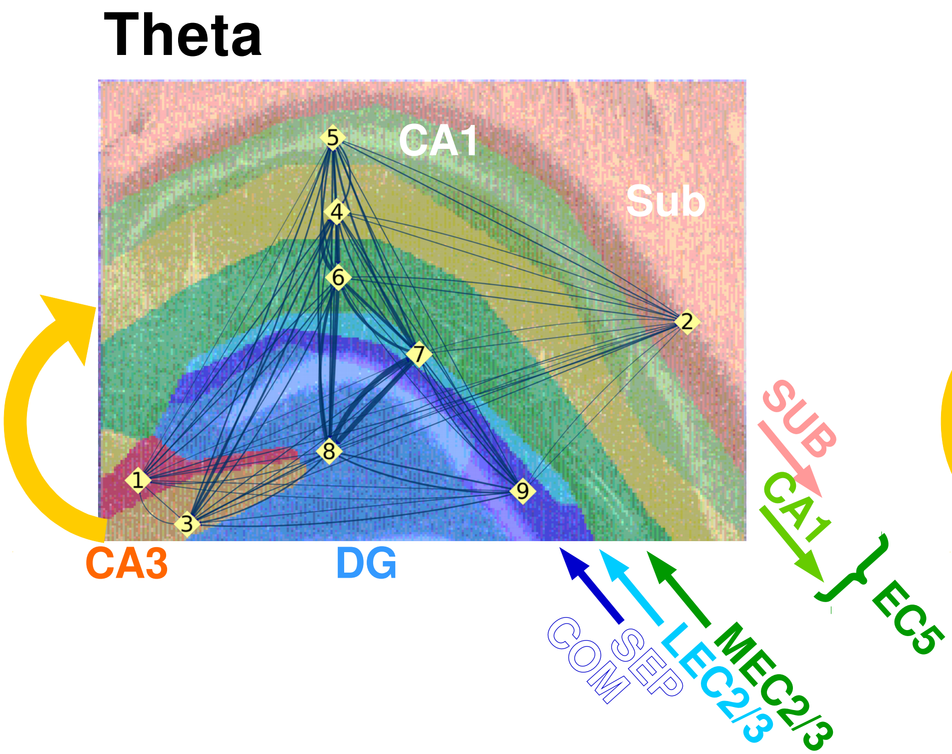

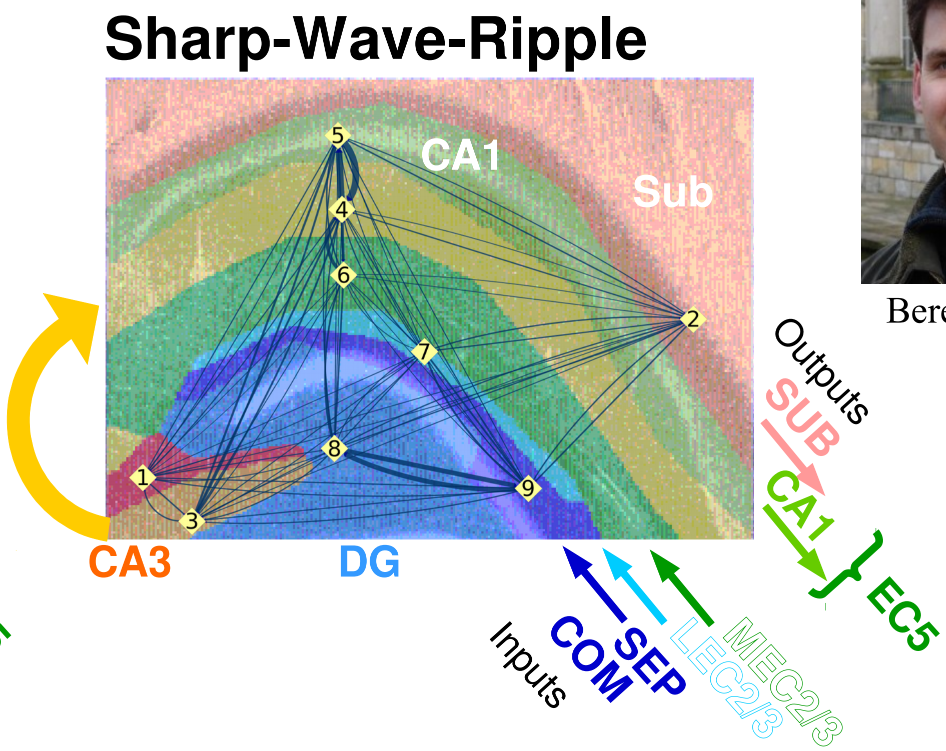

Berényi Antal

Applying Sugihara's causality analysis method to the layer mean CSD, we showed, that there were significant changes in the causal connections between layers and subfields of the hippocampus, between theta and SPW-R. Thickness of the dark blue lines show the connection strength. During theta oscillation, the granular layer of DG were driven by the outer two third of the str. moleculare, (entorhinal perforant path). In contrast, during sharp-wave, the inner third of the str. moleculare (septal and commissural input) was shown to drive the granular and hilar layers. Parallel, the causal connection between CA1 str. lacumosum-moleculare and str. Radiatum is much stronger during theta, while the connection between CA1 rad and pyr is much stronger during SPW-R. The method were more sensitive to the more direct and bidirectional dendritic-somatic connections, than the connections through axon bundles, but relative changes could be high in those cases as well.

Causality between the hippocampal layers

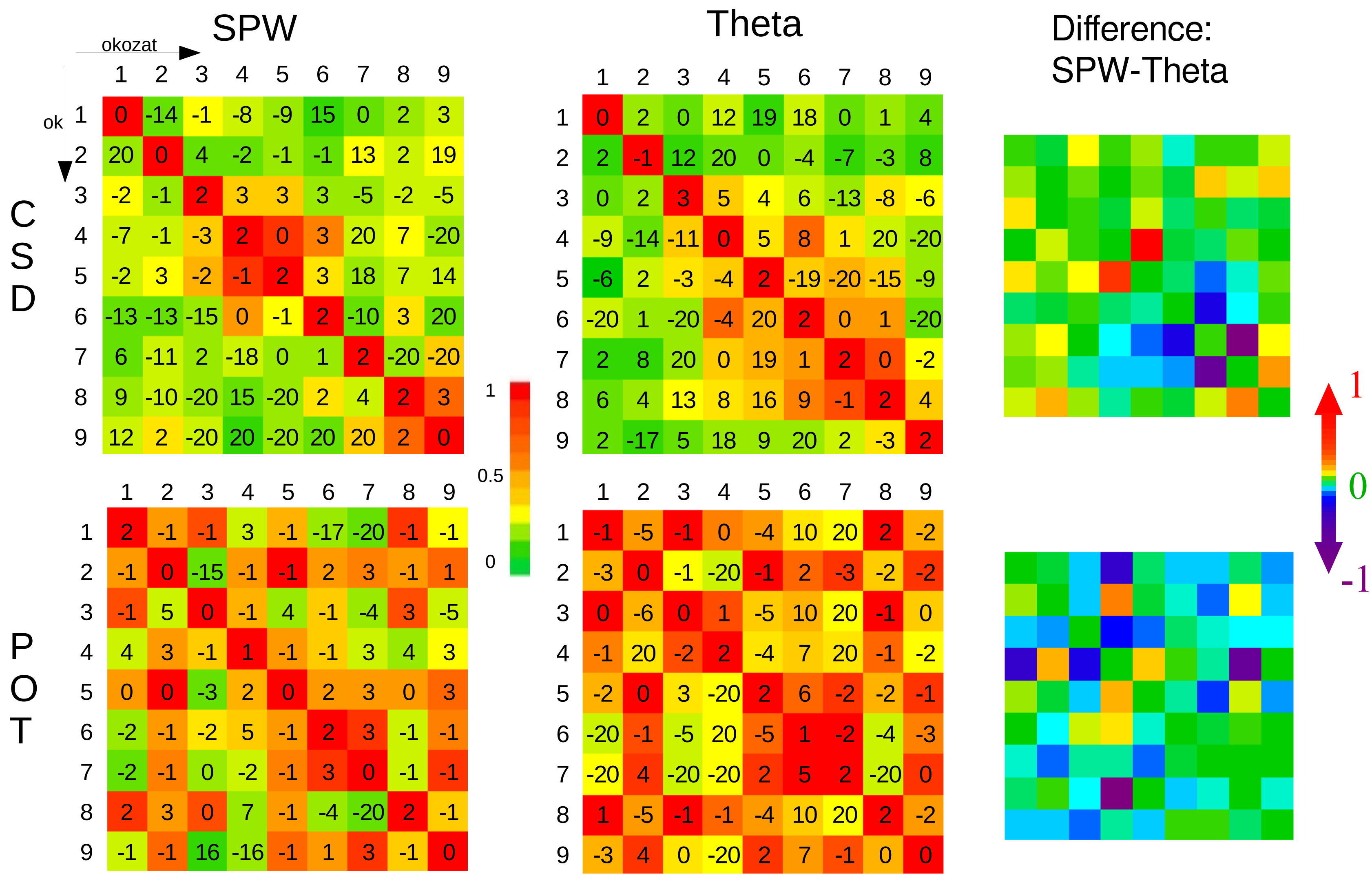

Causality analysis on LFP was quite useless, presumably because of the electric crosstalk. In contrast CSD channels were much more independent and applicable for causality analysis. While the color shows the connection strength, numbers in the boxes show the delay of the effect in time step (using 2kHz subsampled data)

Summary I.

- A new causality analysis method was extended to be by time and delay dependent
- It was tested on simulated time series and applied to different types of neural data.
- In vitro slice preparation during evoked epileptic activity, the causal effect from LFP towards the IOS was captured, although the sampling frequency was 500 times lower for IOS than LFP.
- The delay time of causal effect did not corresponds to the peaks of the cross correlation functions, actually the correlation was negligible at the delay time of the causal effect.
- Based on the causality analysis, a formula was developed describing the temporal evolution of the of the IOS and its dependence on LFP.

Summary II.

- In human epileptic patients foramen ovale recordings, abrupt changes appeared in the connection structures at the initiation of the seizure.

- The connection patterns were conservative through different seizures.

- Some intra hippocampal connections stopped working at the seizure onset, while the majority of the intra hippocampal connections spread along the hippocampus and get stronger. Inter hippocampal connections dropped down during seizure.

Revealing hidden common cause

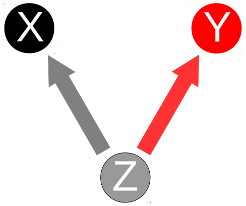

Neither Granger's nor Sugihara's method is able to detect the existence of a hidden common cause or distinguish it from the direct interaction.

We have developed a new method which can!

It is based on the joint dimension measure:

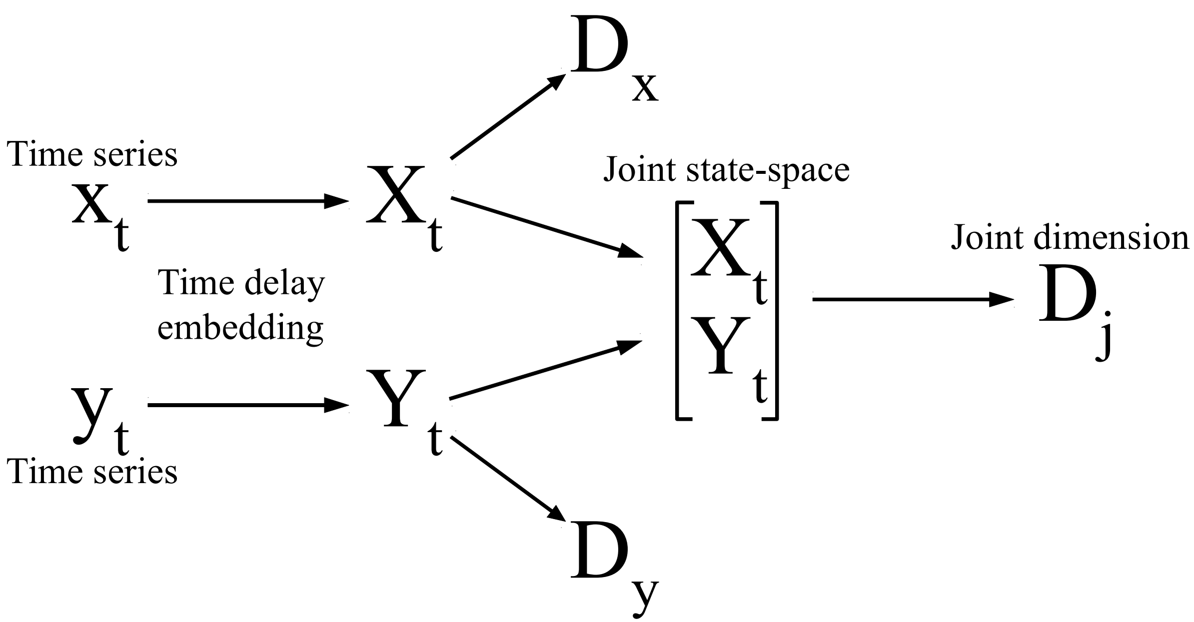

Zsigmond Benkő

Ádám Zlatniczky

András Telcs

How to measure the dimension of the manifold?

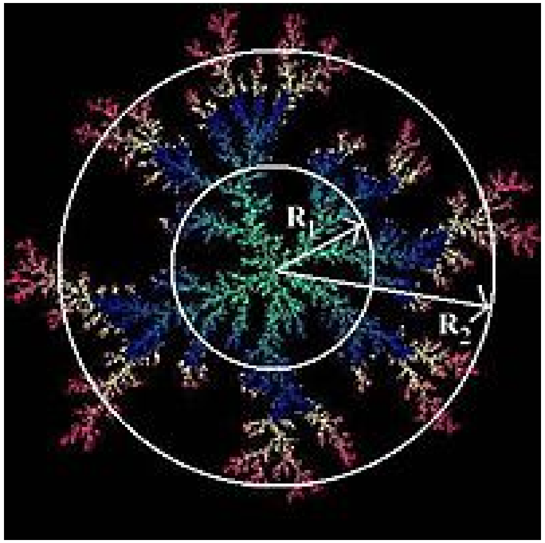

$$N(r) = N_0 \cdot r^D$$

$$D = \frac{Ln\left(\frac{N_i}{N_{i+1}}\right)}{Ln\left(\frac{r_i}{r_{i+1}}\right)}$$

Let’s take two radii and count the number of points within the spheres: the exponent of the increase with respect to the radius gives us the dimension.

Revealing hidden common cause

Key point: the cause does not increases the dimension of the consequence in the joint space, the information is already there!

$x_{n+1}=r_x x_n((1-x_n)+b_{yx}y_n)$

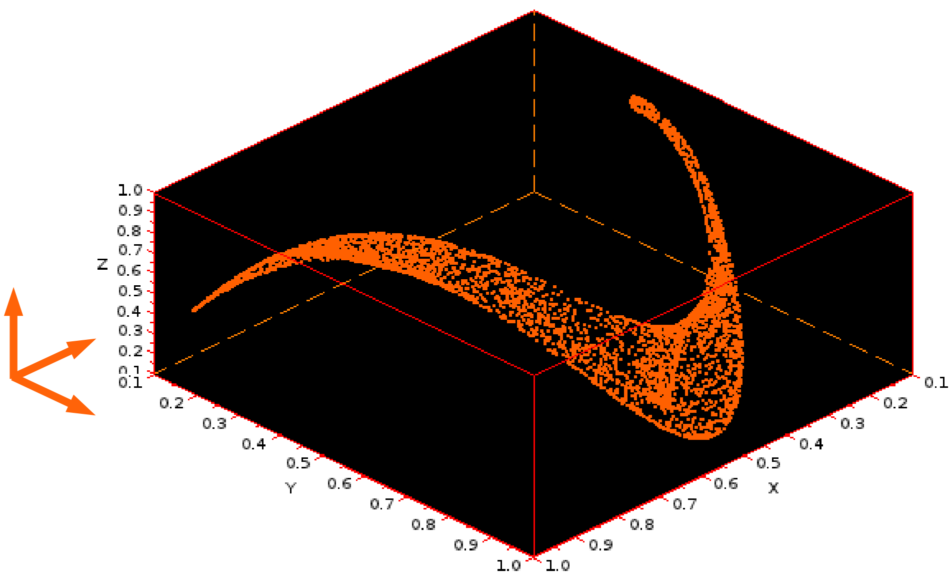

$[x_n;x_{n+1};x_{n+2}]$

The consequence

$y_{n+1}=r_y y_n(1-y_n)$

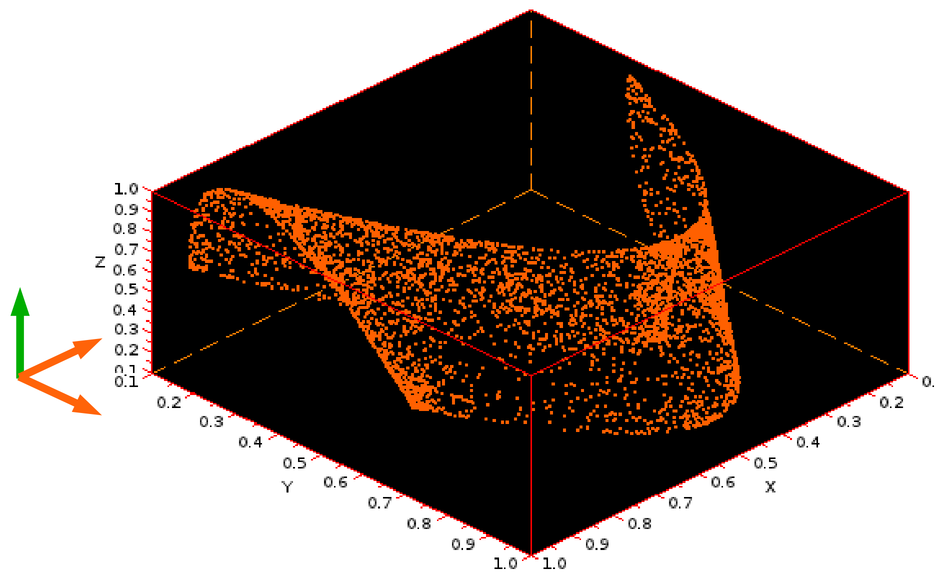

$[x_n;x_{n+1};y_n]$

The cause and the consequence together in the joint space

The consequence formed a 2D manifold both in its own and the together with the cause in the joint state space. The lack of dimensionality increase in the joint dimension is the sign of the existing causal link (x depends on y).

Revealing hidden common cause

$x_{n+1}=r_x x_n((1-x_n)+b_{yx}y_n)$

$y_{n+1}=r_y y_n(1-y_n)$

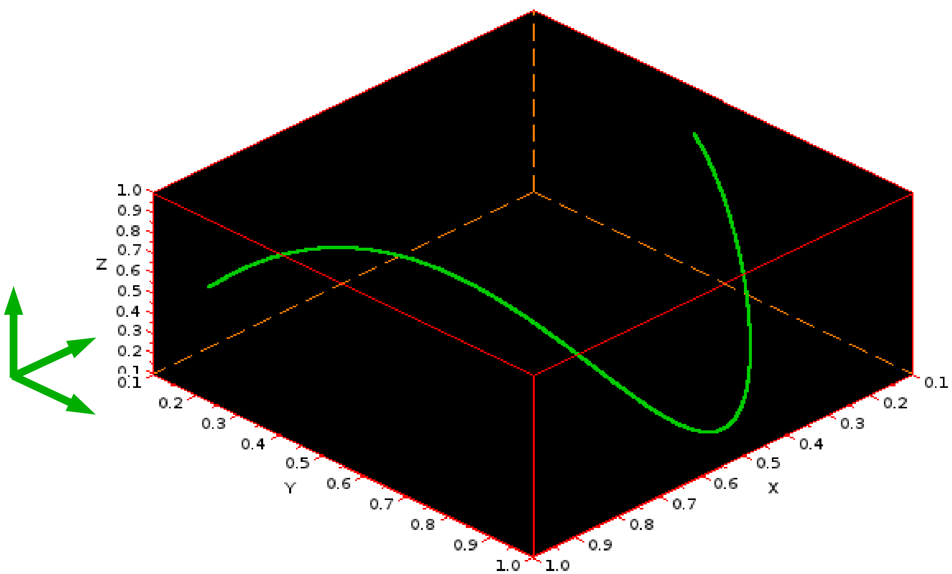

$[y_n;y_{n+1};y_{n+2}]$

The cause

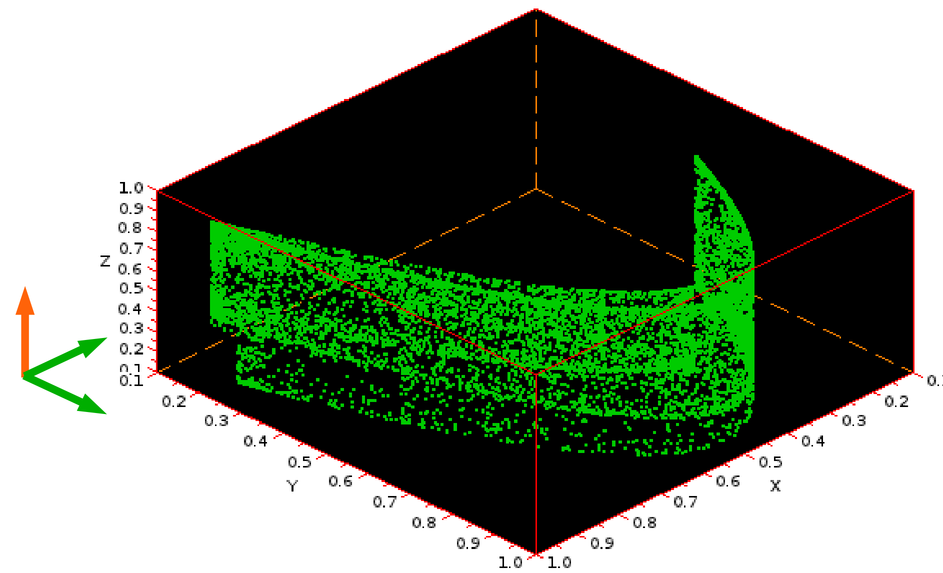

$[y_n;y_{n+1};x_n]$

The cause and the consequence together in the joint space

The cause formed a 1D manifold in its own, but a 2D manifold together with the consequence in the joint state space. The dimensionality increase in the joint state space is the sign of the independence (x contains different information compared to y, thus x does not cause y).

Revealing hidden common cause

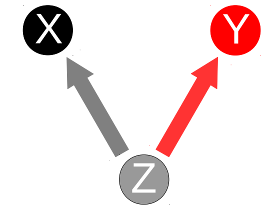

Causal cases and the relations between the single and the joint dimensions:

Independence: $x_t \perp y_t \;\Rightarrow\; D_j = D_x + D_y$

Unidirectional causality: $x_t \rightarrow y_t \;\Rightarrow\; D_j = D_y < D_x + D_y$

Circular causality: $x_t \leftrightarrow y_t \;\Rightarrow\; D_j = D_x = D_y$

Common cause: $x_t \cdots y_t \;\Rightarrow\; Max(D_x, D_y) < D_j < D_x + D_y$

The type of the causal connection can be revealed by measuring the relations between the joint and the individual dimensions.

Test I. Coupled logistic maps

1 - Time-delay embedding

2 - Joining manifolds

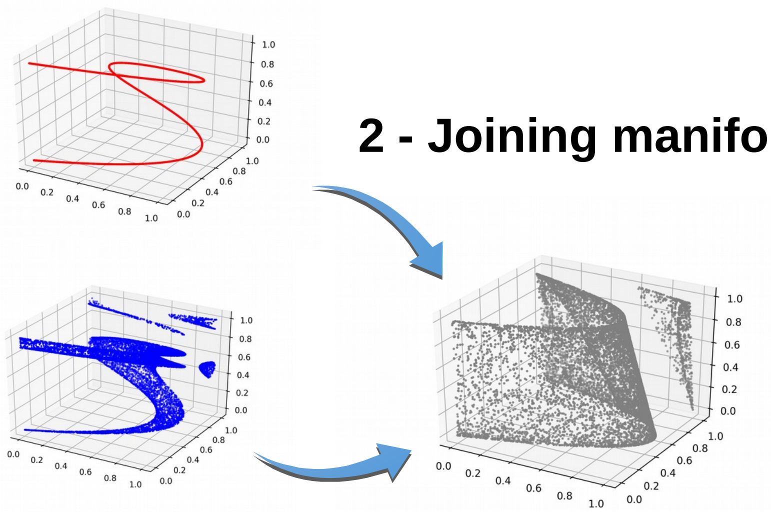

3 - Estimating dimensions

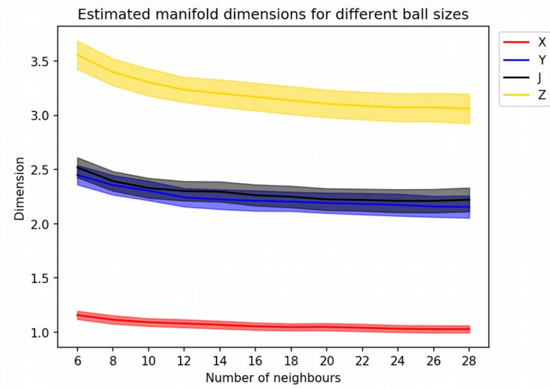

4 - Bootstrapping

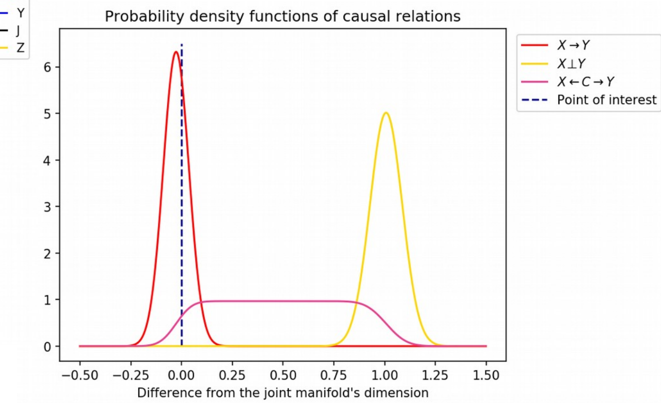

6 – Calculating causal relation probabilities

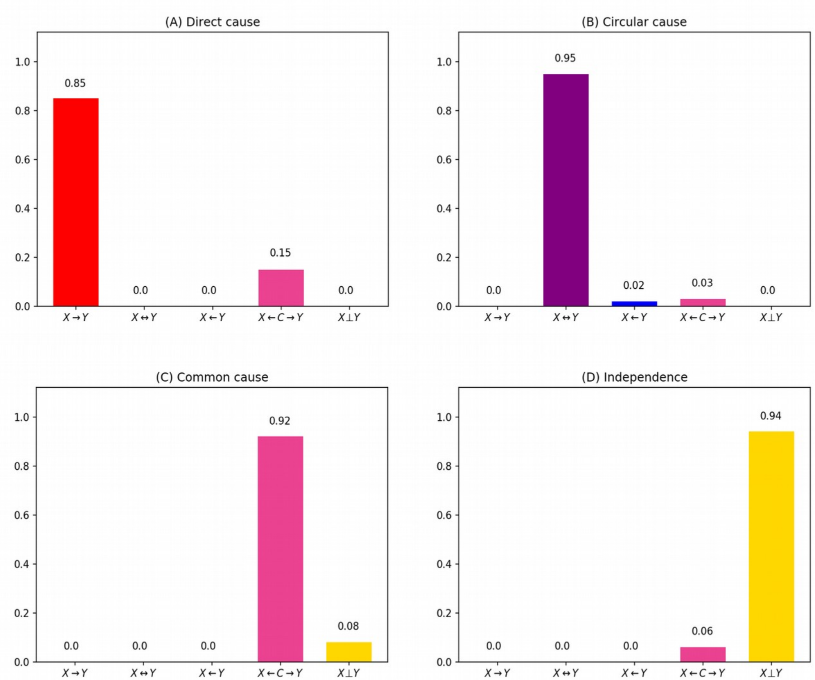

5 - Calculating conditional probabilities

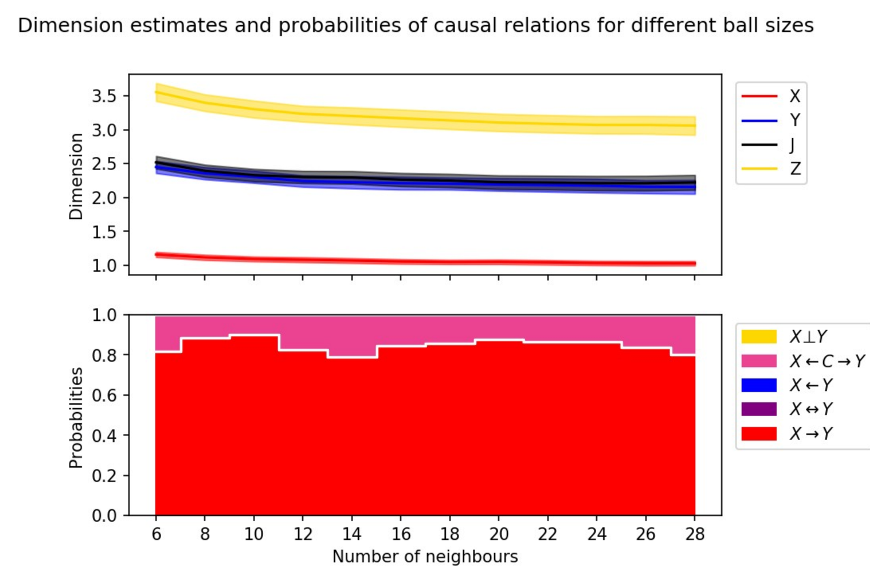

Test II. Coupled Lorentz systems

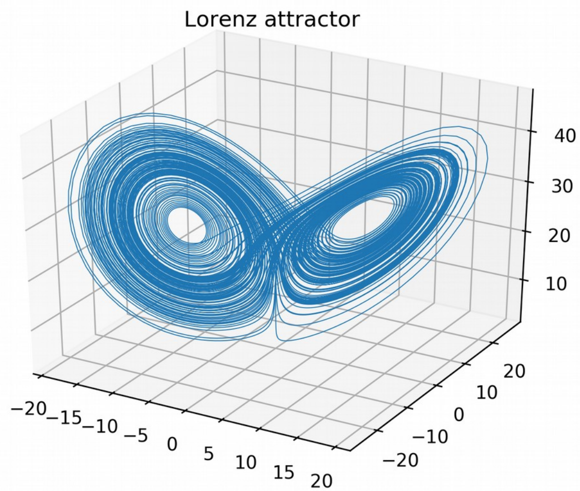

- 3 Lorenz systems: *X, Y, C*
- Each subsystem has 3 coordinates
- They are related through the first coordinates by a coupling

The system is defined by the following differential equations:

$$\dot{x}_1 = \sigma(x_2 - x_1) + m_{y\to x}(x_2 - y_1) + m_{z\to x}(x_2 - z_1)$$
$$\dot{x}_2 = x_1(\rho - x_3) - x_2$$
$$\dot{x}_3 = x_1 x_2 - \beta x_3$$

$$\dot{y}_1 = \sigma(y_2 - y_1) + m_{x\to y}(y_2 - x_1) + m_{z\to y}(y_2 - z_1)$$
$$\dot{y}_2 = y_1(\rho - y_3) - y_2$$
$$\dot{y}_3 = y_1 y_2 - \beta y_3$$

$$\dot{c}_1 = \sigma(c_2 - c_1)$$
$$\dot{c}_2 = c_1(\rho - c_3) - c_2$$
$$\dot{c}_3 = c_1 c_2 - \beta c_3$$

Causal relation probabilities

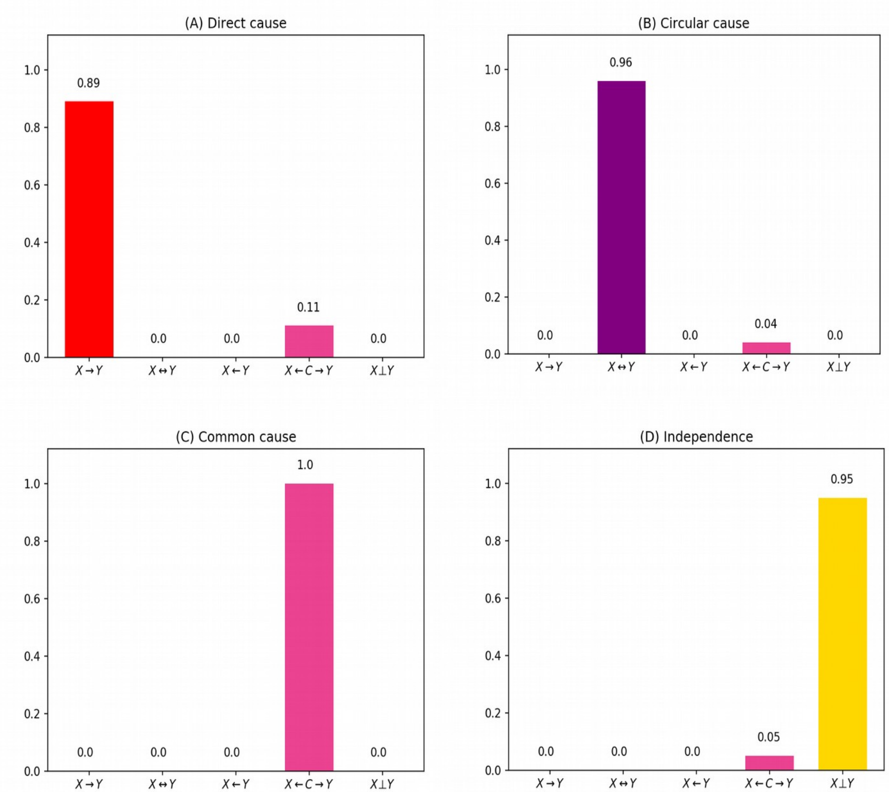

Test III. Analysis of EEG during fotostimulation

- **We computed the CSD at P3 and P4 (didn't use Pz)**
- **Analyzed the concatenated stimulation periods**

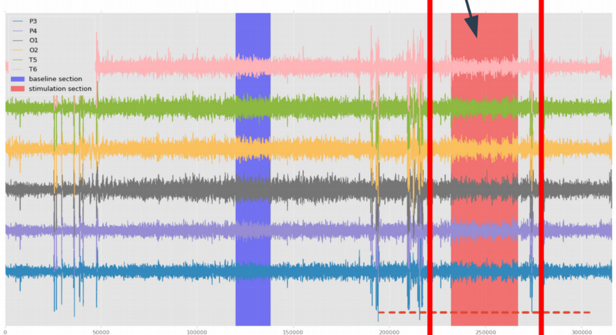

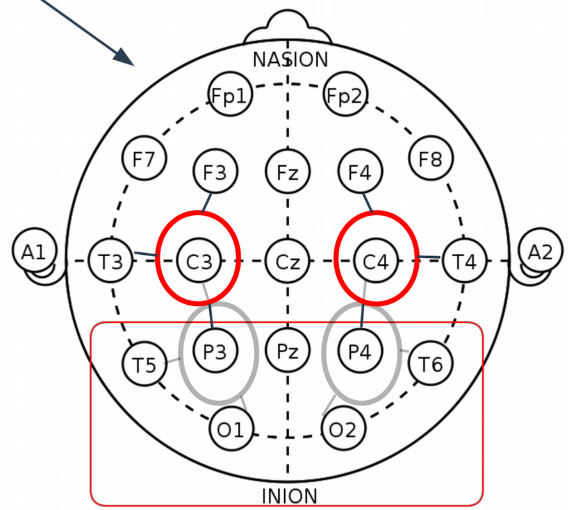

During baseline there was an unidirectional coupling from C4 to C3.

While during stimulation, the analysis resulted in common cause

baseline

stimulation

D=9

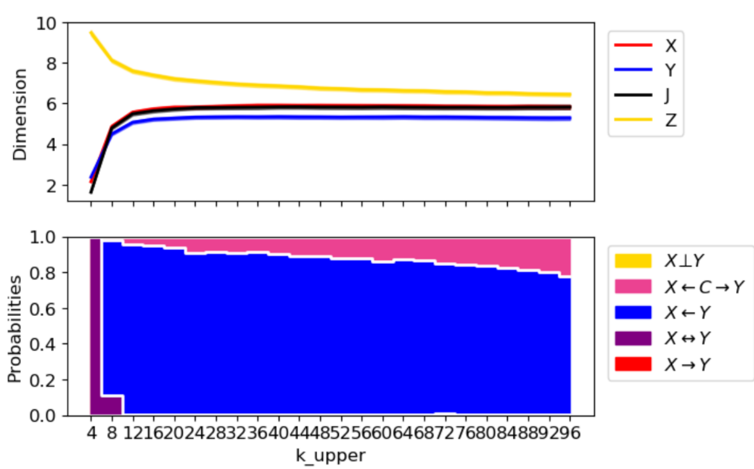

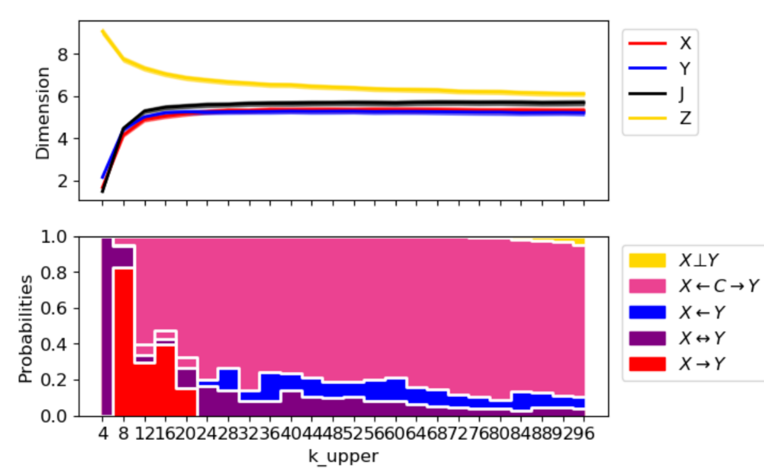

Preliminary application: localization the origin of the epilepsy

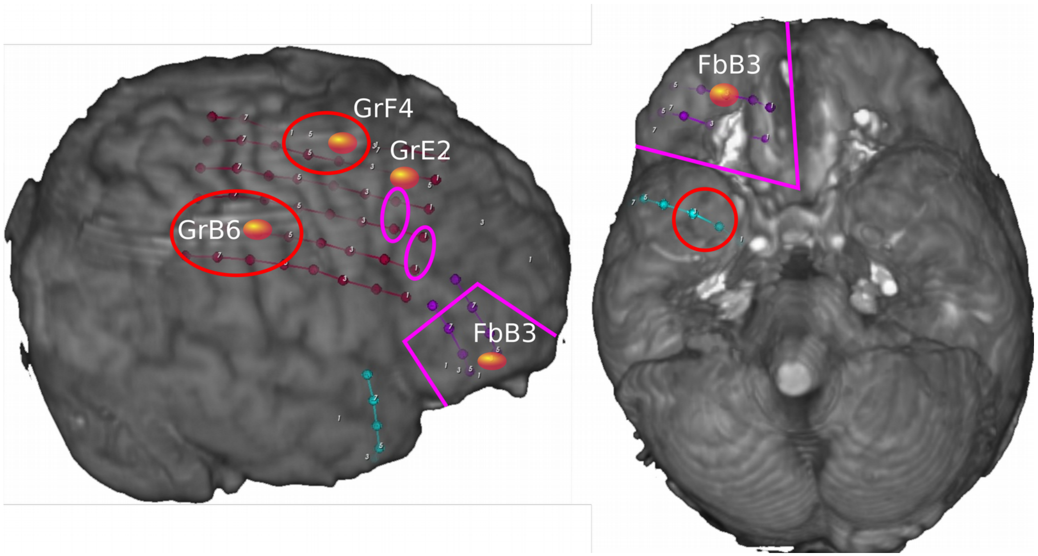

The 20-year-old patient suffered from a drug resistant epilepsy with frequent seizures.

The finding of a cortical dysplasia (at GrF4 electrode site) raised the possibility of the surgical treatment

GrB6 and GrF4 were only slightly involved (red ellipses). Based on the pronounced seizure activity, and the sensitive position of GrB6, only the frontal and orbitobasal parts were cut (purple signs).

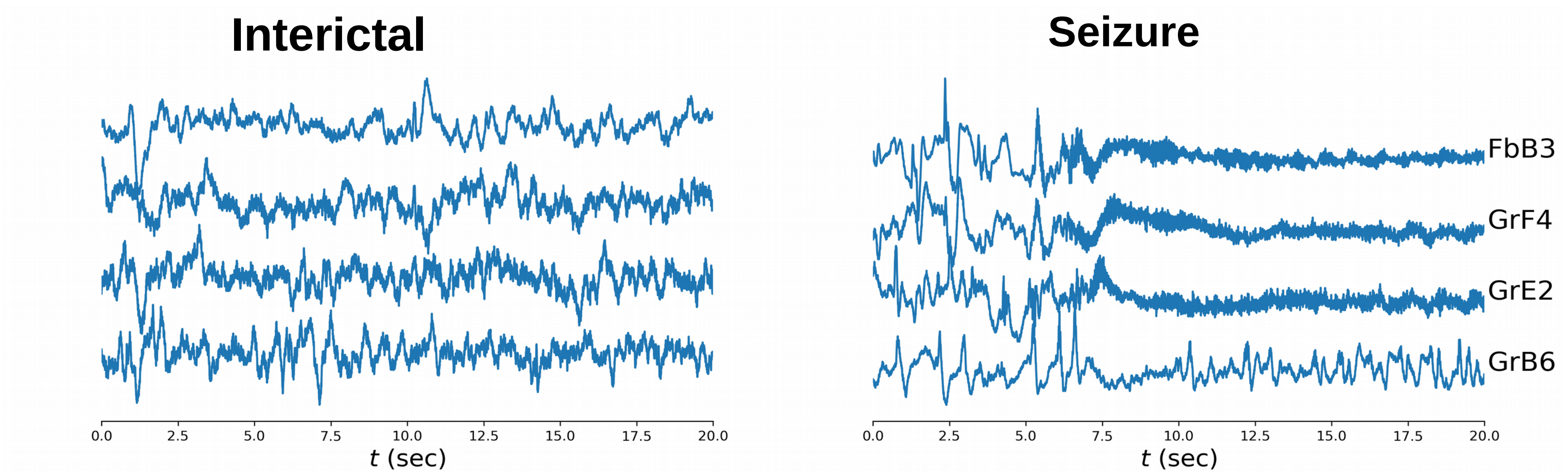

Preliminary application: localization the origin of the epilepsy

Connection probabilities during **interictal** period

GrB6

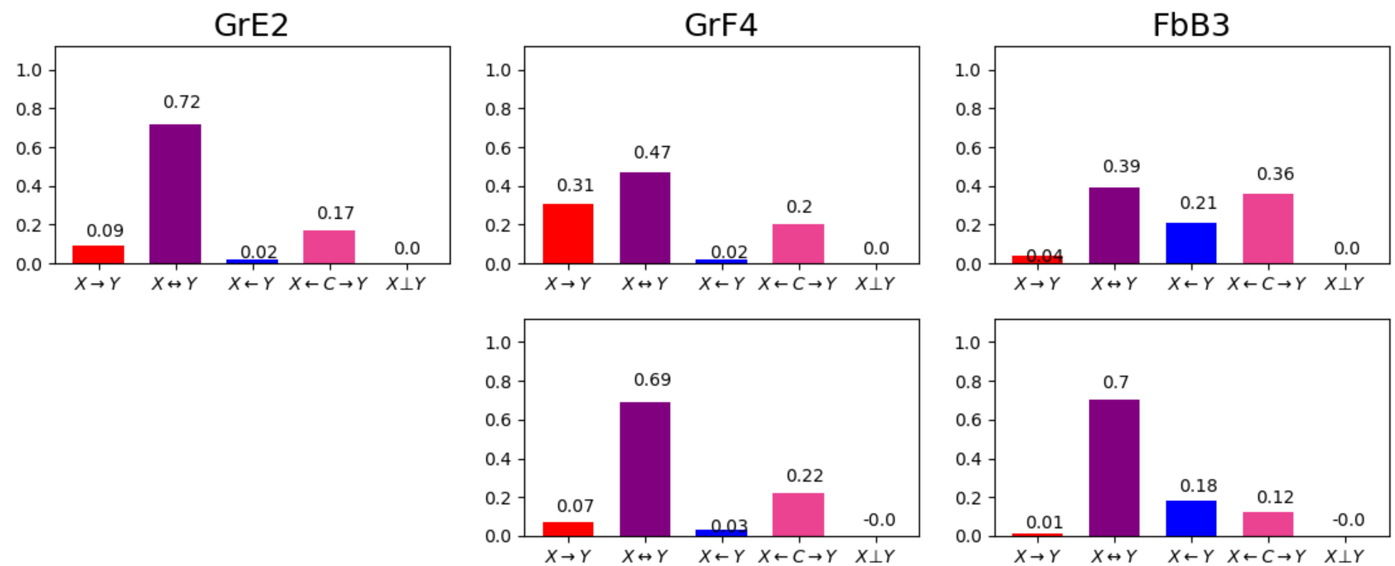

GrE2

GrF4

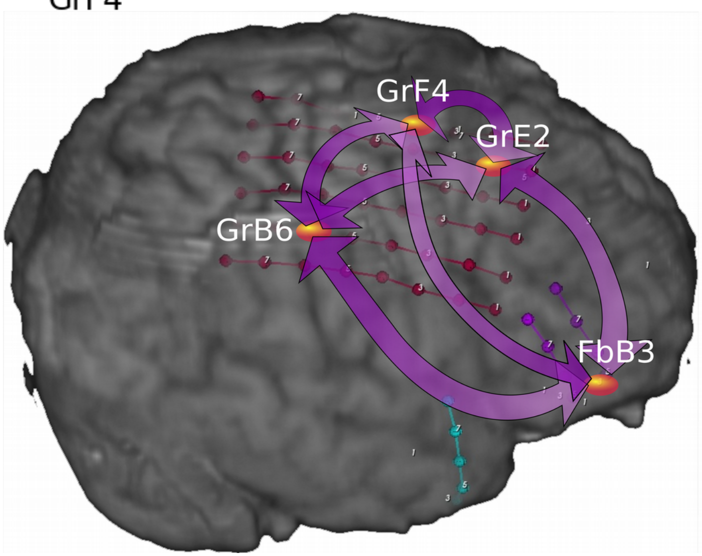

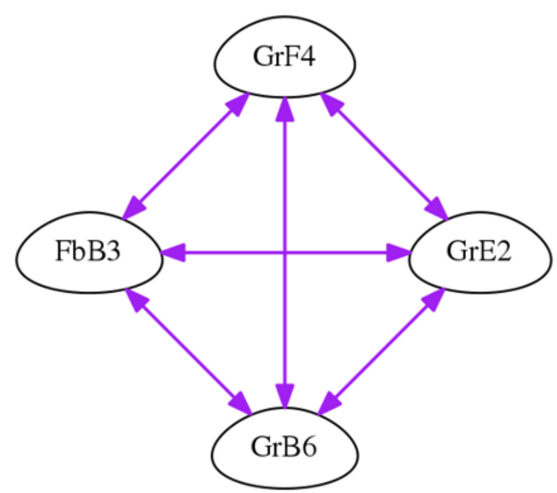

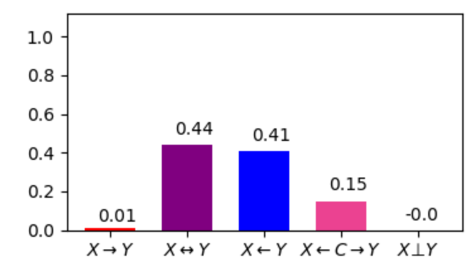

Preliminary application: localization the origin of the epilepsy

Connection probabilities during **ictal** period

GrB6

GrE2

GrF4

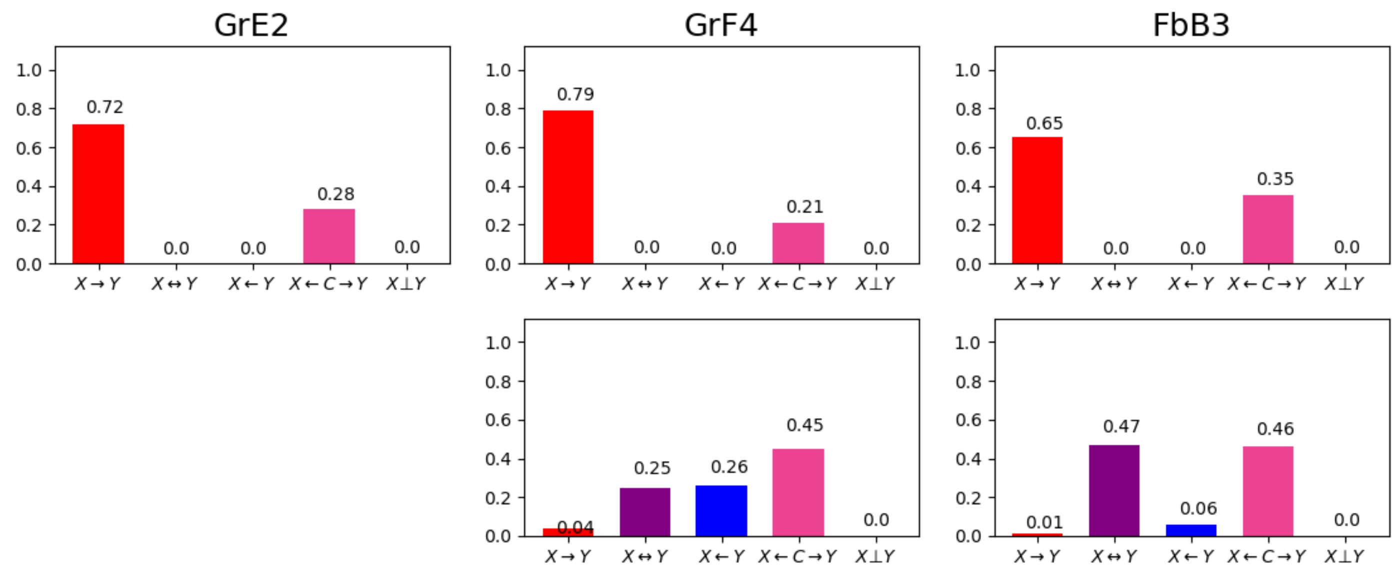

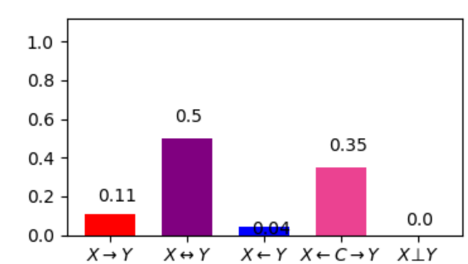

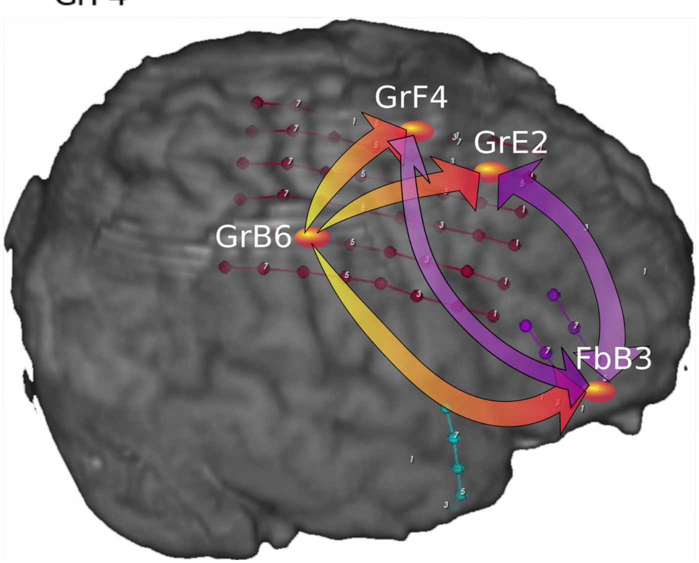

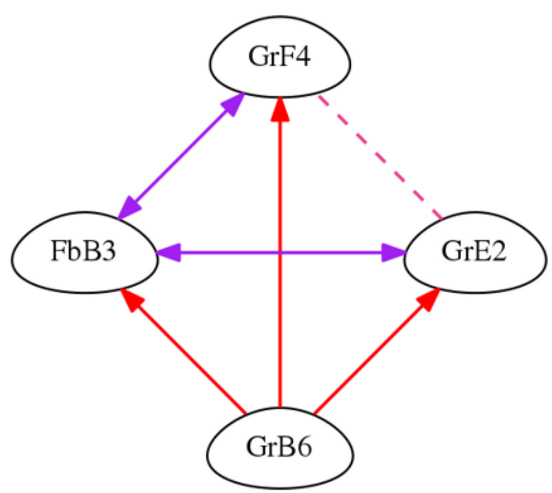

Theoretical Neuroscience and Complex Systems Research Group

Acknowledgement

Péter Érdi

Fülöp Bazsó

László Négyessy

Dorottya Cserpán

László Zalányi

Zsigmond Benkő

This research was supported by grants NKFIH K113147

KTIA_ NAP_13-1-2013-0001

HBP CANON NKFIH NN118902

Thank you for your attention!